

1  
2       **Metamorphosis of memory circuits in *Drosophila* reveal a strategy for**  
3       **evolving a larval brain.**

4  
5       **James W. Truman<sup>1,2</sup>, Jacquelyn Price<sup>1</sup>, Rosa L. Miyares<sup>1</sup>, Tzumin Lee<sup>1</sup>**

6  
7       <sup>1</sup>Janelia Research Campus, H.H.M.I., Ashburn, VA; <sup>2</sup>Friday Harbor Laboratories, University  
8       of Washington, Friday Harbor, WA 98250.

9  
10      **Abstract**

11       Insects like *Drosophila* produce a second brain adapted to the form and behavior of a  
12       larva. Neurons for both larval and adult brains are produced by the same stem cells (neuroblasts)  
13       but the larva possesses only the earliest born neurons produced from each. To understand how a  
14       functional larval brain is made from this reduced set of neurons, we examined the origins and  
15       metamorphic fates of the neurons of the larval and adult mushroom body circuits. The adult  
16       mushroom body core is built sequentially of  $\gamma$  Kenyon cells, that form a medial lobe, followed by  
17        $\alpha'\beta'$ , and  $\alpha\beta$  Kenyon cells that form additional medial lobes and two vertical lobes. Extrinsic  
18       input (MBINs) and output (MBONs) neurons divide this core into computational compartments.  
19       The larval mushroom body contains only  $\gamma$  neurons. Its medial lobe compartments are roughly  
20       homologous to those of the adult and same MBONs are used for both. The larval vertical lobe,  
21       however, is an analogous “facsimile” that uses a larval-specific branch on the  $\gamma$  neurons to make  
22       up for the missing  $\alpha'\beta'$ , and  $\alpha\beta$  neurons. The extrinsic cells for the facsimile are early-born  
23       neurons that trans-differentiate to serve a mushroom body function in the larva and then shift to  
24       other brain circuits in the adult. These findings are discussed in the context of the evolution of a  
25       larval brain in insects with complete metamorphosis.

26  
27      **Introduction**

28       *Drosophila*, like other insects with complete metamorphosis, makes two different  
29       brains during its lifetime: one that functions during its larval stage and the other in the  
30       adult. Such holometabolous insects evolved from direct developing ancestors  
31       (hemimetabolous), which produce only a single brain that functions both in the growing  
32       nymphal stages and in the reproductive adult. Even circuits involved in adult-specific  
33       behaviors such as flight and oviposition are in place at hatching in these insects and their  
34       component neurons change little, except for size from hatching to adulthood (reviewed in  
35       Truman, 2005). How then did this single brain arrangement evolve into a two-brain  
36       system seen in *Drosophila*? The central brain of the fly larva has only about ten percent of  
37       the neurons found in the adult. This numerical difference results from a global arrest of  
38       neurogenesis that occurs during embryogenesis, thereby allowing a much shorter time to  
39       hatching as compared to direct developing insects but resulting in a nervous system with  
40       vastly fewer neurons than found in a hemimetabolous nymph.

42 While producing such a “mini-brain” is in line with a simplified larval body plan, the  
43 truncation of neurogenesis poses challenges for generating the diversity of neuron types  
44 needed to make a CNS. It was shown almost 40 years ago (Thomas *et al.*, 1984) that insects  
45 have an ancient and highly conserved ground plan for making their nervous system.  
46 Neuronal cell types are generated in a modular fashion, with each neural stem cell, called a  
47 neuroblast, generating a characteristic lineage of neuron types, with no crosstalk between  
48 lineage modules (Taghert & Goodman, 1984). Neuronal identity is established within each  
49 lineage through a common temporal code, based on relative birth order (Doe, 2017;  
50 Miyares & Lee, 2019; Rossi *et al.*, 2021). The evolution of the larval nervous system then  
51 occurred within the context of these spatial and temporal mechanisms.

52 The arrays of neuroblasts in both the central brain (Urbach & Technau, 2003) and  
53 ventral nerve cord (VNC) (Thomas *et al.*, 1984; Truman & Ball, 1998) are highly conserved  
54 throughout the insects. For the earliest-born neurons, the relative timing of when different  
55 cell types arise within a lineage is similar in both flies and direct-developing insects like  
56 grasshoppers (e.g., Thomas *et al.*, 1984; Jacobs & Goodman, 1989). Consequently, an early  
57 truncation of neurogenesis leaves the larva with only early-born cell types with which to  
58 make its nervous system.

59 The problem, then, is how does the larva manage to make a complex brain from this  
60 reduced number of cell types? One strategy would be to evolve a new set of temporal rules  
61 for making the larval neurons and then “resetting” the system at hatching and making new  
62 neurons for the adult CNS. However, an analysis of the genes involved in temporal identity  
63 do not show a reset at hatching (Tsuji *et al.*, 2008), and, while some larval neurons do die  
64 at metamorphosis, most larval neurons, especially those in the brain, persist through  
65 metamorphosis and are used again in the adult (Truman, 2005; Roy *et al.*, 2007). Some of  
66 these neurons have similar functions in both larva and adult, as shown by the  
67 demonstration that interneurons causing backward crawling in the larva also control  
68 backward walking in the adult (Lee & Doe, 2021). However, as evident in the present  
69 study, other neurons have profoundly different functions in the two life stages.

70 While there have been numerous studies describing how individual neurons change  
71 through metamorphosis (e.g., Truman & Reiss, 1976; Levine & Truman, 1985; Roy *et al.*,  
72 2007), they do not reveal why some neurons maintain their function while other radically  
73 change as they progress from larva to adult. We decided to examine the metamorphic fates  
74 of the assemblage of neurons that provide the input and output for the mushroom bodies.  
75 This brain region is specialized in both larva and adult to associate odors with either rewards or  
76 punishments and to adjust the animal’s future behavior accordingly (Cognigni, *et al.*, 2018;  
77 Thum & Gerber, 2019). Moreover, the wiring diagram of the mushroom body circuitry is known  
78 at the EM level for both the larva [Eichler *et al.*, 2017] and adult [Zheng *et al.*, 2017; Li *et al.*,  
79 2020]. In direct developing insects like crickets, the mushroom bodies are assembled during  
80 embryogenesis, with different neuron types being produced as embryogenesis progresses  
81 (Malaterre *et al.*, 2002). However, the early arrest of neurogenesis in *Drosophila*, results in only

82 the earliest of these cell types being available for making the larval mushroom bodies. We find  
83 that this temporal constraint underlies the diversity of functional changes that are seen during  
84 metamorphosis.

85

## 86 **Results**

### 87 **The structure and metamorphosis of the Mushroom Bodies.**

88 The core of the *Drosophila* mushroom body is a set of hundreds (larva) to thousands  
89 (adult) of small neurons called Kenyon cells (Fig 1A). Their dendrites form the calyx neuropil,  
90 which receives olfactory input from the antennal lobes, and their bundled axons extend down the  
91 peduncle and into the vertical and medial lobes. The larva has only  $\gamma$  Kenyon cells, which are  
92 born during embryogenesis and the first half of larval life. These neurons have bifurcated axons  
93 that form the larval vertical and medial lobes. Early in the last larval stage, the mushroom body  
94 neuroblasts switch to making  $\alpha'\beta'$  Kenyon cells and then, at the start of metamorphosis, to  $\alpha\beta$   
95 Kenyon cells (Lee *et al.*, 1999). The latter two types of neurons also have bifurcated axons with  
96 vertical and medial branches, but they remain immature until metamorphosis. At the start of  
97 metamorphosis, the  $\gamma$  neurons prune back their axon branches and then regrow only the adult  
98 medial branch, while the  $\alpha'\beta'$  and  $\alpha\beta$  neurons undergo their maturation (Lee *et al.*, 1999;  
99 Awasaki & Ito, 2004). Consequently, the adult mushroom body has three major classes of  
100 Kenyon cells, the  $\gamma$ , the  $\alpha'\beta'$ , and the  $\alpha\beta$  neurons, whose axons form three medial lobes ( $\gamma$ ,  $\beta'$ ,  $\beta$ )  
101 and two vertical lobes ( $\alpha$ ,  $\alpha'$ ).

102 The mushroom bodies mediate olfactory learning *via* the set of extrinsic input and  
103 output neurons that innervate the peduncle and lobes (Fig 1B). In both larvae and adults, these  
104 input and output neurons divide the lobes into non-overlapping, functional compartments, that  
105 have a common microcircuit motif (Fig 1C,D) (Eichler *et al.*, 2017; Zheng *et al.*, 2018). Each  
106 compartment is defined by the axonal tuft of an aminergic input cell which synapses onto  
107 Kenyon cell axons and onto a dedicated output neuron(s). The Kenyon cell axons synapse onto  
108 each other, onto the output cell and back onto the input cells. The majority of the mushroom  
109 body input neurons (MBINs) are dopaminergic neurons (DANs) but a few are octopaminergic  
110 neurons (OANs). The DANs come from two clusters, one that generally encodes reward (the  
111 PAM cluster) and the other that mainly encodes punishment (the PPL1 cluster) (Saumweber *et*  
112 *al.*, 2018; Cognigni *et al.*, 2018; Eichler *et al.*, 2017). The functions of the mushroom body  
113 output neurons (MBONs) from the various compartments are complex because of extensive  
114 interconnections between MBONs and feedback from MBONs back to MBINs. Generally,  
115 however, the output from the PPL1-supplied compartments direct avoidance behavior, while that  
116 from PAM innervated compartments results in attraction (Thum & Gerber, 2019; Cognigni *et al.*,  
117 2018). The larval mushroom body has ten compartments (Saumweber *et al.*, 2018), while the  
118 adult has 16 (Aso *et al.*, 2014) (Fig. 1C). In both stages, the PAM cluster neurons innervate  
119 primarily the medial lobe compartments, while the PPL1 neurons innervate the vertical lobe and  
120 peduncle compartments (Cognetti *et al.*, 2018; Thum & Gerber, 2019).

121        Output from the compartments is by MBONs that release either acetylcholine, GABA or  
122        glutamate. As seen in Fig 1C, in both larva and adult, output from vertical lobe compartments is  
123        typically by cholinergic MBONs while that from medial lobe compartments is typically by  
124        glutaminergic MBONs. The compartments of the peduncle and base of the lobes have either  
125        GABAergic or cholinergic MBONs.

126        With their shortened embryogenesis, *Drosophila* larvae hatch with only  $\gamma$  neurons. To  
127        accommodate the lack of  $\alpha'\beta'$  and  $\alpha\beta$  neurons, these neurons grow a larval-specific vertical  
128        axon branch to form a vertical lobe. A functional mushroom body, though, also requires the  
129        appropriate types of input and output neurons (Tanaka *et al.*, 2008; Aso *et al.*, 2014; Saumweber  
130        *et al.*, 2018). Armstrong *et al.* (1998) used a set of enhancer-trap lines to follow subsets of  
131        extrinsic and intrinsic mushroom body neurons through metamorphosis and showed that some  
132        neurons functioned in both the larval and adult medial lobes. Our use of a large collection of  
133        split-GAL4 lines that express in specific larval MBINs and MBONs (Saumweber *et al.*, 2018)  
134        and a conditional flip-switch strategy (Harris *et al.*, 2015) have allowed us to follow the fates of  
135        most of the extrinsic cells through metamorphosis. We find that some regions of the mushroom  
136        body persist with largely the same components through metamorphosis while other regions are  
137        disassembled and rebuilt with new components for the adult.

138

### 139        **Metamorphic fates of the larval MBINs and MBONs**

140        We focused on the uni-compartmental cells with well-defined dendritic or axonal “tufts”  
141        that define each larval compartment. Following the convention of Veverysa & Allan (2013), we  
142        make a distinction between neurons that undergo remodeling (but stay in the mushroom body  
143        circuit) and those that undergo “trans-differentiation”. We have only morphological criteria for  
144        trans-differentiation and have given this designation to any MBIN or MBON that leaves the  
145        mushroom body to function elsewhere in the adult brain.

146        Fig. 2 and Table 1 summarize the fates of the larval MBINs (Saumweber *et al.*, 2018).  
147        We lacked suitable lines for the two octopaminergic neurons that innervate the calyx  
148        compartment (OAN-a1 &-a2). These cells have a very similar anatomy to the two adult OA-  
149        VUM2a neurons (Busch *et al.*, 2009), leading us to posit that they are the same neurons. The  
150        remaining larval MBINs either remodel, trans-differentiate, or degenerate (Fig 2B,C). Those  
151        innervating the contiguous LP, LA, and LVL compartments typically remain as uni-  
152        compartmental MBINs and innervate similarly positioned compartments in the adult. The  
153        metamorphosis of the octopaminergic MBIN, OAN-g1, is atypical in this group because in its  
154        larval form it is a uni-compartmental neuron that innervates only the LVL compartment, while  
155        its adult form, known as OA-VPM3, continues to have mushroom body contact in the  $\gamma 2$   
156        compartment but also has extensive arbors in the fan-shaped body and the medial and lateral  
157        superior protocerebrum (Busch *et al.*, 2009; Figure 2---figure supplement 1).

158        The larval MBINs in the more distal compartments of the medial or vertical lobes either  
159        trans-differentiated or die. Using our flip-switch approach, we were not able to find adult  
160        counterparts for the four PAM cluster neurons innervating the medial lobe compartments (SHA,

161 UT, IT and LT). As shown in the next section, this failure is because they degenerate at the start  
162 of metamorphosis. The remaining MBINs, which innervate the larval peduncle and distal  
163 vertical lobe compartments trans-differentiate (Figure 2C). The most extreme change was seen  
164 for MBINs-b1 and -b2; they withdraw from the upper peduncle of the larva and subsequently  
165 become sexually dimorphic neurons that innervate the adult optic lobes (Figure 2Cg; Figure 2---  
166 figure supplement 2A,B). In their adult form, they are members of the adult PAL cluster of  
167 aminergic neurons (Mao & Davis, 2009) and we have named them PAL-OL. The three vertical  
168 lobe MBINs (OAN-e1, MBIN-e2, and DAN-f1) are members of the PPL1 group (Saumweber *et*  
169 *al.*, 2018). We did not have a line that allowed us to determine the fate of MBIN-e2. OAN-e1  
170 reorganizes to innervate the neuropil shell surrounding the mushroom body lobes (as PPL1-SMP;  
171 Figure 2---figure supplement 2C) and DAN-f1 forms bilateral arbors in the adult superior medial  
172 protocerebrum as PPL1-bi-SMP (Figure 2--- figure supplement 2D). The remaining MBIN is  
173 MBIN-11 which provides input from the lateral accessory lobe to the larval LA compartment, but  
174 then trans-differentiates to become neuron LAL>bi-CRP that bilaterally innervates the adult  
175 crepine neuropil (Figure 2Bk; Figure 2---figure supplement 2E).

176 We had lines that allowed us to establish the fates of 14 of the 17 types of larval MBONs  
177 (Figure 3; Table 1). None died; the larval cells either remodeled or trans-differentiated. The two  
178 cells from the larval calyx (MBON-a1 & -a2) illustrate two extremes of remodeling (Figure  
179 3Ca,b). The larval MBON-a2 neuron assumes a very similar anatomy in the adult where it is  
180 called MBON 22 (AKA MBON-calyx). By contrast, the larval MBON-a1 neuron leaves the  
181 calyx and is redirected to the  $\gamma$  lobes as the adult neuron MBON 29 (AKA MBON  $\gamma 4\gamma 5$ ). The  
182 larval MBONs innervating peduncle or vertical lobe compartments (IP, LP, UVL, IVL and LVL)  
183 either leave the mushroom bodies altogether (Figure 3Cg,h,j) or, like MBON-e2 and -f2, shift to  
184 medial adult lobe compartments (Figure 3Cd,e). Our flip-out approach did not give us the adult  
185 identity of MBON-c1, which projects from the larval LP compartment, but its early metamorphic  
186 outgrowth is directed into the calyx (Fig 3Cj; see next section). By contrast to the MBONs  
187 innervating the larval vertical lobe and peduncle compartments, those innervating the medial  
188 lobe remain as medial lobe neurons in the adult and supply topologically similar compartments  
189 (Figure 3m-r).

190 The fates of the neurons that undergo trans-differentiation vary markedly. For example,  
191 MBON-b1 and -b2 leave the larval IP compartment and become local interneurons in the adult  
192 lateral horn (Figure 3Ch; Figure 3---supplementary figure 1B) (LHNL neurons; Dolan *et al.*,  
193 2019). The most striking changes occur in MBON-g1 and -g2 (Figure 3Cg; Figure 3---  
194 supplementary figure 1C,D), which transform into the LAL.s-NO2i.b neurons that innervate the  
195 nodulus of the adult central complex (Wolff & Rubin, 2018).

196

## 197 The time-course of transitions of larval mushroom body extrinsic neurons

198 The fates of most of the larval input and output neurons that we determined by the flip-  
199 switch method were confirmed by following the expression of the parental lines through early  
200 metamorphosis (Figures 4, 5). Many enhancer-based lines change their expression patterns in

201 the transition from larva to adult, but we found that GFP expression typically persists through  
202 enough of the remodeling period to confirm the cell's adult identity.

203 As expected by our failure to find the adult forms of DAN-h1 to -k1 using the flip-switch  
204 method, we found that all four neurons degenerated early in metamorphosis (Figure 4G,H).  
205 Their dendritic arbors collapsed by 8 hr after puparium formation (APF), cell bodies were  
206 disrupted by 18 hr APF, and, by 24 hr APF, they were reduced to scattered GFP-labeled debris.

207 The remaining MBINs and MBONs either remodeled or trans-differentiated (Figures 4  
208 & 5) and they showed a time-course of pruning and outgrowth that paralleled changes in the  $\gamma$   
209 Kenyon cells. Pruning of  $\gamma$  neuron axons is evident by 4 hr APF and is completed by 16 to 18 hr  
210 APF (Watts *et al.*, 2003). Adult outgrowth then commences by 24 hr and is finished by 48 hr  
211 (Yaniv *et al.*, 2012; Mayseless *et al.*, 2018). All MBINs (Figure 4) and MBONs (Figure 5)  
212 showed arbor loss by 8 hr APF and were completely pruned by 16 hr APF. Growth cones  
213 became evident between 16 and 24 hr APF. MBIN-b1 & -b2 showed the most exuberant  
214 outgrowth, having formed growth cones that were halfway to the optic lobes by 16 hr APF and  
215 reaching these structures by eight hours later (Figure 4A and supplementary figure 1). Most  
216 neurons achieved their adult form by 48 hr APF. The APL and MBON-j2 neurons were  
217 exceptional in their outgrowth because they continued arbor extension beyond 48 hr (Fig. 4I and  
218 5L). APL eventually covers all of the adult compartments by 72hr APF (Mayseless *et al.*, 2018)  
219 and provides inhibitory feedback from the lobes to the calyx. For MBON-j2, its  $\gamma 4$  tuft formed at  
220 the same time as those of other MBONs but the formation of its  $\gamma 2$  and especially its  $\gamma 1$  arbors  
221 was delayed. (Figure 5---supplement figure 1). In its adult function as MBON 05 (AKA MBON-  
222  $\gamma 4 > \gamma 1, \gamma 2$ ), it provides feed-forward inhibition from  $\gamma 4$  to  $\gamma 2$  and  $\gamma 1$  (Aso *et al.*, 2016). Its  
223 extended period of outgrowth may allow time for the compartment microcircuits to become  
224 established before it interconnects them.

225 MBON-a1 and -a2 provide an interesting contrast of divergent remodeling of two similar  
226 larval cells (Figure 5A,B). Both cells were retracting their dendritic and axonal arbors by 8 hr  
227 APF. MBON-a1 completely removed its dendritic arbor by 16 to 24 hr, and the distal portion of  
228 the neuron extended new growth to innervate the  $\gamma 4$  and  $\gamma 5$  compartments and surrounding  
229 neuropils. In contrast, the dendritic arbor of MBON-a2 only partially regressed, organized into a  
230 dendritic growth cone by 16 to 24 hr APF, and reinvaded the calyx. In its adult form as MBON-  
231 20 (MBON-calyx; Aso *et al.*, 2014; Li *et al.*, 2020), its dendritic and axonal arbors are very  
232 similar to its former larval form.

233 The most stable extrinsic neuron is DAN-d1. Its dendritic arbor remained intact through  
234 metamorphosis and its axonal tuft underwent a mild, transient thinning from 8 to 18 hr APF and  
235 then extended fine processes into the forming  $\gamma 2$  and  $\alpha' 1$  compartments between 24 and 48 hr  
236 APF (Figure 4D). A more extreme remodeling was evident in MBON-d1 (Figure 4E). Its larval  
237 dendritic tuft retracted and reorganized into a growth-cone by about 18 hr APF, extended into the  
238  $\gamma 1$  and peduncle compartments by 24 hr, and achieved its adult dendritic configuration by 48h.  
239 Its axonal arbor expanded from a compact projection in the larva to a sparse arbor along the adult  
240  $\alpha$  and  $\beta$  lobes (Aso *et al.*, 2017; Li *et al.*, 2020).

241 Amongst the cells undergoing trans-differentiation, the most extreme changes were seen  
242 in MBON-g1 & g2, which shifted from the larval mushroom body to the adult central complex  
243 (Figure 5H). Their larval axonal arbors were retracting by 8 hr APF and organized into an  
244 axonal growth cone by 18 hr APF. The growth cone then navigated medially to innervate the  
245 intermediate zone of the nodulus. The dendritic tufts of MBON-g1 & -g2 thinned by 8 hr APF  
246 and then fragmented as new dendritic growth cones sprouted from the base of the old arbor (18  
247 hr APF). The dendrites invaded and expanded to cover the ipsilateral lateral accessory lobe. A  
248 similar level of extreme change between larval and adult morphologies was seen for MBIN-b1  
249 and b2 that became sexually dimorphic, optic lobe input interneurons in the adult (Figure 2 –  
250 figure supplement 2A,B).

251 MBON-c1 was refractory to the flip-switch approach, but its early metamorphic changes  
252 gave us insight into its adult function. As seen in Figure 5 – figure supplement 2, by 24 hr APF  
253 its larval dendritic arbor was essentially gone, and new growth cones have invaded the calyx.  
254 This line lost its GFP expression after this time but the extensive growth into the calyx by 24 hr  
255 indicates that this neuropil is its terminal, adult target. Its anatomy at 24 hr APF, though, was too  
256 immature to match it to any known adult cell, so we have called its adult form MBEN-CA  
257 (mushroom body extrinsic neuron to calyx).

258

### 259 **The larval form is a derived state for the neurons that show trans-differentiation**

260 For trans-differentiating neurons, that assume two different identities, is one identity  
261 ancestral for the cell and the other identity derived to accommodate metamorphosis?  
262 Establishing such homologies is difficult for the extrinsic neurons but it is possible for neuron  
263 groups in the VNC, such as the midline spiking interneurons (Figure 6). These neurons are  
264 found in a large cluster in each thoracic hemineuropil and each cluster is the progeny of a single,  
265 identified neuroblast (Shepherd & Laurant, 1984). Their cell bodies lie near the ventral midline  
266 and they project to the contralateral leg neuropil where they shape the response of leg  
267 motoneurons to input from leg mechanoreceptors (Siegler & Burrows, 1984). They were first  
268 described in grasshoppers (Siegler & Burrows, 1984) but they are found in both direct  
269 developing and metamorphic insects (Witten & Truman, 1998), indicating an involvement in leg  
270 circuitry through insect evolution.

271 In *Drosophila*, these inhibitory neurons arise from the neuroblast NB4-2 during the  
272 postembryonic phase of neurogenesis (Harris *et al.*, 2015; Lacin & Truman, 2016). They are  
273 stockpiled as immature cells during larva growth and then mature into midline inhibitory  
274 interneurons at metamorphosis. The embryonic-born neurons of this lineage (e.g. neurons T13s,  
275 T13t, T13u and T13v2; Figure 6A), however, are commissural interneurons that look nothing  
276 like their postembryonic siblings. However, as shown in Figures 6B and C, at metamorphosis  
277 these neurons trans-differentiate to assume the same terminal identity as the postembryonic-born  
278 cells. Therefore, we see that just like in the direct developing grasshopper (Shepherd & Laurant,  
279 1984), *Drosophila* starts producing its midline leg interneurons during embryogenesis but the  
280 early-born cells initially take on an **assumed** identity adapted to larval needs and defer

281 expressing their ancestral identity as leg interneurons until metamorphosis. This comparison  
282 between direct developing and metamorphosing insects, then, argues that the adult identity of a  
283 trans-differentiating neuron represents its ancestral identity while its assumed identity in the  
284 larva is a derived identity that evolved to accommodate the highly modified larval stage. The  
285 significance of this relationship will be considered below.

286

### 287 **Origins of adult-specific Mushroom Body input and output neurons.**

288 Remodeled larval MBINs and MBONs do not account for all of the input and output  
289 neurons of the adult mushroom bodies (Figures 2B and 3B). The adult has about 40 different  
290 types of MBINs and MBONs (Aso *et al.*, 2014; Li *et al.*, 2020) and we found that only 15 types  
291 also function in the larval structure. The remaining 25 types could either come from other trans-  
292 differentiating neurons whose larval function is outside of the mushroom bodies or they could be  
293 born during the postembryonic neurogenic period. The origins of 22 of these 25 types are  
294 summarized in Figure 7A,B and Table 2. They are all postembryonic born. We found no neuron  
295 whose terminal fate was as a mushroom body extrinsic neuron but assumed a different function  
296 in the larva.

297 The MBIN side of the adult circuit is dominated by the addition of about 150 PAM-class  
298 neurons divided into at least 15 different types (Aso *et al.*, 2014; see also Lee *et al.*, 2020; Li *et*  
299 *al.*, 2020). These neurons are born during the postembryonic phase of neurogenesis and come  
300 from the CREa1A and CREa2A lineages (Lee *et al.*, 2020) (Table 2). This massive addition of  
301 PAM cluster neurons suggests an enhanced sophistication for discriminating rewarding stimuli in  
302 the adult versus the larva (e.g., Li *et al.*, 2020). By contrast, there is no change in the number of  
303 PPL1 neurons that primarily provide input to the compartments involved in aversive  
304 conditioning. While the number remains constant, though, the cell population partially changes:  
305 the adult adds three new PPL1 neurons to the set (Ren *et al.*, 2016), but loses three larval PPL1  
306 neurons to other brain circuits of the adult (Figure 2).

307 For the MBONs, the origins of nine of the twelve remaining types (Table 2; Fig 7B) were  
308 determined using the twin-spot MARCM technique (Yu *et al.*, 2009). As seen in Fig. 7C,  
309 MBONs 12 (also called MBON- $\gamma 2\alpha'1$ ), 13 (MBON- $\alpha'2$ ), and 14 (MBON- $\alpha 3$ ) are born in  
310 succession during the postembryonic divisions in the FLAa2 lineage. Most of the remaining  
311 vertical lobe MBONs arise in the DL1 lineage (Fig 7D; Table 2). DL1 is a Type II neuroblast  
312 that has an atypical division pattern (Boone & Doe, 2008; Wang *et al.*, 2014). Each neuroblast  
313 division produces an intermediate precursor cell which, in turn, produces a small series of  
314 ganglion mother cells. Each of the latter divides to make two daughter neurons. As shown in  
315 Figure 7D for a number of these ganglion mother cells, one daughter becomes a vertical lobe  
316 MBON while the other becomes a central complex neuron, innervating the fan-shaped body.

317

## 318 **Discussion**

### 319 **Strategies for generating neurons for the larval CNS**

320 Our analysis of the metamorphosis of the mushroom body has revealed at least five  
321 strategies for producing larval neurons (Figure 8A). The **first** strategy is that a neuron acquires  
322 its terminal identity during embryogenesis. It has similar form and function in both larva and  
323 adult although there may be some remodeling of arbors going from one stage to the other. DAN-  
324 d1, for example, shows little change from larva to adult. Its dendritic arbor remains largely  
325 intact through metamorphosis while its axonal tuft shows only a moderate thinning before re-  
326 expanding (Figure 4D). MBON-j1 provides a more typical pattern. Its larval and adult forms  
327 are quite similar, but the larval cell still goes through severe axonal and dendritic pruning but  
328 then regrows into a very similar morphology for the adult (Figure 5K).

329 The pruning of larval neurons at metamorphosis is caused by a global, hormonal signal --  
330 the ecdysone surge that drives metamorphosis (Lee *et al.*, 2000; Schubiger *et al.*, 1998). Local,  
331 extrinsic factors, though, can also influence the extent of pruning (Williams and Truman, 2005).  
332 The importance of such factors for pruning in the mushroom body circuit was shown by studies  
333 on the APL neuron (Mayseless *et al.*, 2018). APL pruning is dramatically suppressed by the  
334 selective inhibition of axon degeneration in the  $\gamma$  Kenyon cells, the major synaptic partner of this  
335 neuron. The remodeling of MBINs may have a similar dependence on the state of their  
336 postsynaptic targets. The  $\gamma$  Kenyon cells prune back their axons from the distal compartments but  
337 retain some processes in the LP and LA compartments at the base of the lobes. In parallel, the  
338 MBINs to the latter two compartments (i.e., DAN-c1 and -d1) show only moderate pruning  
339 (Figure 4B,D: P+16h and P+24h), while those innervating more distal compartments prune  
340 severely and regrow their arbors from defined growth cones (*e.g.*, Figures 4E,F). This pattern  
341 suggests that the severity of axon pruning by the MBINs depends on the extent of loss of their  
342 postsynaptic targets.

343 The quantitative differences seen in the MBINs, though, are not seen in the MBONs. The  
344 latter undergo severe dendritic pruning and regrow from growth cones, regardless of which  
345 compartment they innervate (Figure 5). This difference between MBONs and MBINs suggests  
346 that dendrite pruning may be less dependent on the state of local environments as compared to  
347 axonal pruning.

348 The **second** strategy is that a neuron's larval form is based on the cell arresting its  
349 development at some intermediate point in its trajectory to its terminal identity. This is  
350 analogous to the case of ingrowing thalamic neurons in the developing mammalian forebrain  
351 (Kanold *et al.*, 2003). These early-born neurons arrive prior to the birth of the cortical granule  
352 cells so they initially synapse on subplate neurons. After the granule cells are born, they lose  
353 their connections in the subplate and move into the cortex. A similar scenario in *Drosophila* is  
354 suggested by the two sets of octopaminergic cells, OAN-g1 and OAN-a1 & -a2. We find that the  
355 adult form of OAN-g1 is OA-VPM3 (Fig 2Cf; Busch *et al.*, 2009; Busch & Tanimoto, 2010).  
356 Its adult form has a minor contact with the  $\gamma$ 2 compartment and then branches exuberantly in the  
357 fan-shaped body of the central complex and in the superior medial protocerebrum. The larval  
358 form of the cell, though, stops in the LVL compartment (the larval homolog of  $\gamma$ 2) and only  
359 continues on to the central complex and superior medial protocerebrum at metamorphosis. A

360 similar situation is seen for OAN-a1 & -a2. In their larval form they innervate the antennal  
361 lobes and mushroom body calyx (Figure 2Ca), but their terminal form in the adult extends  
362 beyond the mushroom body to the lateral horn (Busch *et al.*, 2009).

363 The **third** strategy is illustrated by larval neurons that acquire a functionality that is  
364 absent from their terminal identity. The  $\gamma$  Kenyon cells provide an excellent example in that  
365 their larval form possesses a vertical axon branch that is lacking in their adult form. Importantly,  
366 this vertical branch is also absent from  $\gamma$  neurons in species that do not have a larval stage (e.g.,  
367 the cricket; Malaterre, *et al.*, 2002) supporting the idea that it is a larval-specific modification.

368 The **fourth** strategy is trans-differentiation, which provides the neuron with two distinct  
369 identities: its **terminal identity**, which is evident in the adult, and an **assumed identity**, which  
370 is seen in the larva. The most extreme example which we found involved the two pairs of  
371 central complex neurons (LAL.s-NO<sub>2</sub>i.b) that assumed the identities of mushroom body neurons  
372 in the larva (as MBON-g1 and -g2; Fig. 5H). We also found adult optic lobe neurons (Figure  
373 4A) and lateral horn neurons (Figure 5C) that first assumed identities as a mushroom body  
374 extrinsic neurons in the larva. A less extreme identity shift was seen for PPL1-SMP. In its larval  
375 form as OAN-e1, it innervates the Kenyon cell core of the UVL compartment but in its terminal  
376 identity it shifts to the neuropil shell surrounding the vertical and medial lobes (Figure 4C).  
377 Trans-differentiation of neurons through ontogeny is not unique to insect metamorphosis. It is  
378 also seen in developing zebrafish in the case of dorsal root ganglion sensory neurons that  
379 transform into sympathetic neurons after they migrate away from the dorsal root ganglion  
380 (Wright *et al.*, 2010).

381 We do not know if there is a qualitative distinction between cells that remodel versus  
382 those that trans-differentiate or if these just represent the two extremes of a continuum. Some  
383 cells, like MBON-e2 and MBON-j2, have features of both strategies. They function as MBONs  
384 in both larva and adult but their roles within the mushroom body circuitry change. MBON-j2  
385 provides output from a medial lobe compartment to contralateral brain regions outside of the  
386 mushroom bodies while its terminal identity is to provide intercompartmental communication  
387 with the  $\gamma$  lobe (Figure 5L). MBON-e2 makes the opposite shift. Its assumed function in the  
388 larva is to assemble output from multiple vertical lobe compartments while its terminal function  
389 in the adult is as a uni-compartmental MBON in the adult  $\beta'2$  compartment (Figure 5F).

390 The **fifth** strategy is for larval neurons to be recruited from the population of neurons that  
391 normally die during embryogenesis. This is a common strategy in the VNC. Neurons are  
392 generated according to a reiterated segmental plan in the VNC, but in direct developing insects  
393 like grasshoppers, many neurons needed in the thorax are not needed in the abdomen. They are  
394 nevertheless produced in both regions, but segment-specific cell death then removes the  
395 extraneous cells from the abdomen (e.g., Thompson & Siegler, 1993). Larvae, like those of  
396 *Drosophila*, that use abdominal-based crawling for locomotion, though, require many more  
397 abdominal neurons than survive in the abdominal CNS of a grasshopper nymph. These larvae  
398 appear to acquire needed neurons by drawing from this large pool of embryonic abdominal  
399 neurons that are fated to die (Truman, 2005). Their death is delayed so that they can function in

400 the larva but once the larval stages are finished, they revert to their ancestral fate and degenerate.  
401 This use of such phylogenetically “doomed” neurons is common in the abdominal segments but  
402 less prevalent in the larval thorax or the brain. Indeed, of the larval brain neurons in this study,  
403 only the four PAM neurons die after the larval stage is completed (Figure 4G,H). It is curious  
404 that these four neurons die rather than remodeling to join the ~150 new PAM neurons that are  
405 added for the adult (e.g., Lee *et al.*, 2020). It may be that “doomed” neurons such as these are  
406 able to assume a temporary identity that allows them to survive and function in the larva but  
407 must then revert to their terminal fate of degeneration at metamorphosis.

408

#### 409 **Factors related to trans-differentiation**

410 How are neurons selected to undergo trans-differentiation and assume identities for use in  
411 the larval mushroom body circuitry? Besides the observation that many of these neurons are  
412 fated for roles in adult-specific circuits, we find that five of the seven types of trans-  
413 differentiating neurons come from lineages that produce other neurons that are terminally fated  
414 to function in the mushroom bodies (Table 1). The OAN-e1 and DAN-f1 neurons that function  
415 in the mushroom body only in the larva come from the CPd2/3 lineage that also produces the  
416 PPL1 01 (= larval DAN-c1), PPL1 02 (= larval DAN-g1) and PPL1 03 (= larval DAN-d1)  
417 neurons that function in both larval and adult mushroom bodies. The larval MBIN-11 and  
418 MBON-b1, -b2 neurons come from the BLVa3/4 lineage that produces APL, and the larval  
419 MBON-g1 and -g2 neurons come from the DAL-V2/3 lineage that produces MBON 09 and 10  
420 (= larval MBON-h1 and -h2) (Table 1; Saumweber *et al.*, 2018).

421 Two main mechanisms are involved in establishing neuronal identities within a lineage:  
422 are established by: one is the relative timing of birth of the neuron’s ganglion mother cell (Kohwi  
423 & Doe, 2013; Doe, 2017; Miyares & Lee, 2019) and the other is Notch-dependent signaling  
424 between the two siblings from the ganglion mother cell division (Skeath & Doe, 1998). As  
425 summarized in Fig. 8B,C, we speculate that either of these mechanisms could be exploited to  
426 recruit neurons for temporary function in the mushroom bodies.

427 The trans-differentiation of a subset of the PPL1 neurons (Figure 8B) could involve  
428 modifying temporal fate determination within the PPL1 cluster. The larva has seven tyrosine  
429 hydroxylase positive neurons in its PPL1 cluster (Selcho *et al.*, 2009) and these innervate the  
430 core of the larval mushroom body. The adult has twelve neurons in this cluster but, again, only  
431 seven of these innervate its mushroom body core while the remainder target surrounding  
432 neuropils (Mao & Davis, 2009). We find, though, that the seven neurons that innervate the  
433 mushroom body are not all the same in the two stages. The three neurons supplying the larval  
434 vertical lobe leave the mushroom body circuit and join other brain circuits of the adult. They are  
435 replaced by three new PPL1 neurons that are added during the second neurogenic period in the  
436 larva (Ren *et al.*, 2016). Two neuroblasts contribute to the PPL1 cluster in both the larva  
437 (Saumweber *et al.*, 2019) and the adult (Ren *et al.*, 2016). We assume that those innervating the  
438 adult mushroom body likely come from the same neuroblast, although only four of them are born  
439 during embryogenesis and can therefore contribute to the larval circuit. The missing three

440 neurons either come from the other stem cell or by the temporary transformation of other early-  
441 born cells in the DL2 lineage (Figure 8B). Although such genes have not been found for these  
442 neurons, we assume that there are terminal selector genes (Hobert & Kratsios, 2019) that  
443 determine the phenotype of the PPL1 neurons that innervate the mushroom body. We speculate  
444 that the appropriate selector genes may be expressed prematurely in the DL2 lineage to allow  
445 other cells to assume an MBIN identity. For these cells, though, the MBIN selector gene  
446 expression is temporary and lost at metamorphosis, thereby allowing the neurons to switch to  
447 their ancestral fate in the adult.

448 In contrast to the above scenario, the ability of the central complex neurons, LAL.s-  
449 NO<sub>2</sub>i.b, to temporarily assume identities as the larval MBON-g1 and -g2 may involve  
450 suppressing the divergent fates of sibling neurons as depicted in Figure 8C. The two neurons  
451 arising from the division of a ganglion mother cell typically have very distinct terminal identities  
452 with *Notch* signaling determining the difference between the “A” (*Notch*-on) and the “B”  
453 (*Notch*-off) phenotypes (Skeath & Doe, 1998). *Hey* (Hairy/enhancer-of-split like with a Y) is a  
454 bHLH-O protein which is an important *Notch* target for establishing the “A” phenotype  
455 (Monastirioti *et al.*, 2010). Interestingly, *Hey* expression is not *Notch* dependent in the Kenyon  
456 cell lineage (Monastirioti *et al.*, 2010), and in these lineages the two sibling neurons are  
457 identical. We find that sibs that show central complex versus mushroom body fates show up  
458 multiple times in the DL1 lineage (Figure 7D). We speculate that the MBON 09/10 versus  
459 LAL.s-NO<sub>2</sub>i.b phenotypes seen in the DAL-v2/3 lineage represents a similar divergence of  
460 sibling phenotype with one destined for the central complex and the other for the mushroom  
461 body. Alteration of *Notch* signaling in the embryo, though, might allow the neuron destined for  
462 the central complex to temporarily assume characteristics of its mushroom body sibling, thereby  
463 becoming another MBON. At metamorphosis, the latter cell would somehow reverse the altered  
464 *Notch* effects and acquire its terminal identity as a central complex neuron. The scenarios in the  
465 last two paragraphs are quite speculative but suggest possible avenues of research that could be  
466 explored to determine the basis for trans-differentiation.

467 In some of the cases we examined, the interneurons that acquired an assumed identity in  
468 the larva lacked the targets that are appropriate for their terminal identities. In contrast to the  
469 interneurons, the embryonic born motoneurons that lack their adult targets do not seem to have  
470 the plasticity to assume other functions. The indirect flight motoneuron, M5, (Consoulas *et al.*  
471 2002) and the embryonic-born leg motoneurons of lineage 15 (Lacin & Truman, 2016) lack their  
472 normal adult targets in the larva and they remain in an arrested immature state through larval  
473 growth and delay their maturation until metamorphosis. A similar developmental arrest has yet  
474 to be found amongst embryonic-born interneurons. Given the small number of interneurons that  
475 are available to it, the embryo likely uses every interneuron that is available to make its larval  
476 CNS.

477

## 478 **Relationship of cell fate to mushroom body compartments**

479        Based on the analysis of enhancer trap lines, Armstrong *et al.*, (1998) found that larval  
480    extrinsic neurons mainly ended up in the  $\gamma$  lobe compartments of the adult. As seen in Figure  
481    9A, our cell-by-cell analysis of the fates of the larval neurons reached a similar conclusion with  
482    the additional insight that some of the larval cells leave the mushroom bodies at metamorphosis  
483    and function elsewhere in the adult brain.

484        Whether the association of a larval neuron with the mushroom body represents the cell's  
485    assumed or terminal identity relates to the compartment it innervates. Seven of the larval  
486    compartments correspond to the six adult compartments that contain  $\gamma$  cell axons. The larval LP,  
487    LA, LVL and SHA compartments correspond to the adult peduncle,  $\gamma$ 1,  $\gamma$ 2 and  $\gamma$ 3 compartments  
488    respectively. The three larval "toes" (UT, IT, and LT) correspond to compartments  $\gamma$ 4 and  $\gamma$ 5.  
489    The remaining 10 compartments contain axons of the  $\alpha$ ' $\beta$ ' and the  $\alpha$  $\beta$  Kenyon cells and are not  
490    directly homologous to any larval compartments because they have different Kenyon cell cores.  
491    However, the  $\beta$  and  $\beta$ ' compartments share features in common with neighboring adult  $\gamma$   
492    compartments.

493        Figure 9B examines the extrinsic neurons of the larval medial lobe compartments from  
494    the perspective of their terminal identity. On the MBIN side, the larval compartments are  
495    innervated solely by "doomed" neurons that temporarily serve as PAM neurons but then die at  
496    metamorphosis. For the larval medial lobe MBONs, by contrast, they express their terminal  
497    identities at hatching and express the same transmitters and innervate comparable compartments  
498    along the medial lobe axis (Fig. 9B) in both larva and adult.

499        The metamorphic changes for the neurons in the remaining six larval compartments are  
500    variable and summarized in Figure 9C. As described above, the adult peduncle,  $\gamma$ 1 and  $\gamma$ 2  
501    compartments are homologs of the larval LP, LA and LVL compartments, respectively. On the  
502    MBIN side, the three dopamine neurons to these compartments acquire their terminal identity as  
503    DANs by hatching and provide dopamine input in both larva and adult (Table 1). The  
504    octopaminergic MBIN, OAN-g1, innervates the homologous compartment in both larva and  
505    adult (LVL vrs  $\gamma$ 2), but its terminal adult form as OA-VPM3 expands to other targets beyond the  
506    mushroom body. The only stable compartment on the output side is LA (=  $\gamma$ 1); in the larva  
507    MBON-d1 provides GABAergic from LA, and in its adult form of adult MBON 11, this neuron  
508    continues to provide output from the  $\gamma$ 1 and the peduncle compartments. The larval LP and LVL  
509    compartments, by contrast, are supplied by trans-differentiated neurons. MBON-c1 provides  
510    larval-specific cholinergic output from LP and MBON-g1 & -g2 provide GABAergic output  
511    from LVL. The adult-specific MBONs that replace these cells at metamorphosis invert the  
512    transmitter output from these two compartments.

513        The remaining larval compartments, UVL, IVL and IP, have no adult homologs. The  
514    UVL and IVL compartments form a vertical lobe "facsimile" for the larva, thereby substituting  
515    for the lack of  $\alpha$  and  $\alpha$ ' axons and their extrinsic neurons. Their MBINs and MBONs assume a  
516    vertical lobe function for the larva but their terminal destinations are either in the adult medial  
517    lobes or in other parts of the adult brain (Fig.9C).

518        The IP compartment is intriguing because it is innervated by a unique cluster of MBINs  
519 (the PAL cluster) and it has no counterpart in the adult mushroom body. While the nine other  
520 larval compartments are highly interconnected by one- or two-step connections from the MBONs  
521 to the MBINs, the IP MBINs receive no such feedback (Eschbach *et al.*, 2020). Likewise, its  
522 MBONs provide the least amount of crosstalk to the other larval compartments. This circuit  
523 isolation suggests that the IP compartment may be involved in a type of learning distinct from  
524 that handled by other compartments. Since none of its input or output cells have terminal  
525 functions associated with the adult mushroom bodies, the type of learning mediated through the  
526 IP compartment may be unique to the larva.

527        Figure 9D shows that the temporal sequence of birth of the major classes of adult Kenyon  
528 cells is paralleled by the temporal sequence of birth of their respective MBONs and MBINs. We  
529 did not include the medial lobe in this comparison because of the massive postembryonic  
530 addition of the PAM neurons (Figure 7A). The  $\gamma$  Kenyon cells start being produced during  
531 embryogenesis and almost all their MBINs and MBONs are also produced through the same  
532 period. The latter have acquired their terminal identities by the time hatching and innervate the  
533 mushroom body in both larva and adult. By contrast, the  $\alpha'\beta'$  and  $\alpha\beta$  Kenyon cells are born late  
534 in larval life and through metamorphosis (Lee *et al.*, 1999) and we find that they are supplied  
535 primarily by late-born MBONs and MBINs that arise during postembryonic growth and have no  
536 role in the larval structure.

537

### 538 **Changes in mushroom body circuit architecture through metamorphosis.**

539        A goal of this study was to determine the extent that mushroom body circuits were  
540 conserved through metamorphosis. Figure 10A summarizes the compartmental overlap of  
541 MBINs and MBONs in their larval versus adult configurations. There are three MBIN-MBON  
542 pairings that are found in both stages. Not unexpectedly, two involve the multi-compartmental  
543 feedback neuron, APL, which expands to cover all of the compartments in the adult. The last  
544 conserved pairing occurs outside of the lobes, in the calyx. For the uni-compartmental neurons  
545 of the lobe system, though, we found no MBIN-MBON pairings that persisted through  
546 metamorphosis.

547        Besides MBIN to MBON connections, the compartments of both the larva (Eichler *et al.*,  
548 2017; Eschbach *et al.*, 2020) and the adult (Aso *et al.*, 2014; Li *et al.*, 2020) are highly  
549 interconnected, both by MBON to MBON connections and by feedback and feed forward  
550 connections from MBONs back to MBINs. For MBON to MBON interactions, larval (Eichler *et*  
551 *al.*, 2017) and adult (Li *et al.*, 2020) data are available for seven of the MBONs that function in  
552 both circuits (Fig 10B). There are 42 possible pair-wise connections amongst these cells  
553 excluding connections of a MBON onto itself. The MBONs are more highly interconnected in  
554 their adult configuration as compared to their larval one: the adult group shows 13 connections  
555 (31% of possible connections) while in their larval configuration they have seven (17%).  
556 Importantly, only three connections (7%) are common to both configurations. This percentage is  
557 similar to the 5% predicted if the two stages were wired up completely independently at their

558 respective levels. This low level of shared connections suggests that in both configurations the  
559 MBONs are free to interconnect in a way that is optimal for the particular life stage.

560 There are very few direct MBON to MBIN connections in the larva. Rather, connections  
561 between these cells are provided by an extensive network of one- and two-step feedback and  
562 feed forward pathways (Eschbach *et al.*, 2020). We do not know the metamorphic fates of the  
563 neurons of these pathways, so we cannot compare their connectivity in the two stages.

564 The simplest functions of the mushroom bodies are in short-term appetitive or aversive  
565 conditioning and there are examples in both larvae and adults showing that manipulation of the  
566 input or output cell from a single compartment can support or suppress these short-term  
567 processes (e.g., Saumweber *et al.*, 2018; Aso *et al.*, 2012). Although their input-output  
568 relationships do not survive metamorphosis (Figure 10A), single neurons may still have similar  
569 functional roles in both larva and adult, such as diagrammed in Figure 10C. In the adult, the  
570 stimulation of the DAN PPL1 01 (= PPL1-  $\gamma$ 1pedc ) is sufficient to induce short-term aversive  
571 conditioning to a paired odor (Aso *et al.*, 2012; Das *et al.*, 2014). This neuron innervates the  
572 peduncle and  $\gamma$ 1 compartments and acts through the GABAergic output cell MBON-11 (Aso *et*  
573 *al.*, 2012; Aso *et al.*, 2014). The larval form of PPL1 01 is DAN-c1 (Figure 2), but it only targets  
574 the larval LP compartment where it contacts the cholinergic output neuron MBON-c1 (Eichler *et*  
575 *al.*, 2017). Stimulation of DAN-c1 in the larva, though, does not support short-term aversive  
576 conditioning (Eschbach *et al.*, 2020). The larval version of the adult output partner (MBON 11)  
577 is called MBON-d1 (Figure 3). It receives input from DAN-d1 (Eichler *et al.*, 2017), and  
578 stimulation of this DAN-d1 is sufficient to support short-term aversive conditioning in the larva  
579 (Eschbach *et al.*, 2020). Consequently, MBON-d1/ MBON 11 is involved in short-term aversive  
580 conditioning in both larva and adult, but a different dopamine MBIN instructs it in the two  
581 stages.

582 Mushroom bodies of larvae and adult also mediate higher order functions such as long-  
583 term learning, shifts in learning valence dependent on internal state, and the ability to extinguish  
584 or re-consolidate memories (Cognigi *et al.*, 2018; Thum & Gerber, 2019). These higher order  
585 processes involve intra- and intercompartmental connections with feed-forward or feed-back  
586 interactions amongst MBONs or from the MBONs back to the MBINs. Figures 10D-F illustrate  
587 the circuitry underlying three types of higher order networks in the adult and indicate which  
588 components are present in the larva. Memory consolidation continues for minutes to hours after  
589 training and involves recurrent activity within  $\alpha$  lobe compartments. A recurrent loop that is  
590 necessary for memory stabilization after training with a sugar reward involves PAM- $\alpha$ 1 neurons,  
591  $\alpha$  Kenyon cells and the cholinergic MBON- $\alpha$ 1's (Ichinose *et al.*, 2015). Larvae lack all three of  
592 these neuron types, but Eichler *et al.*, (2015) showed that the larval vertical lobe facsimile has  
593 similar circuit motifs that involve feedback of cholinergic MBONs back onto their  
594 compartmental MBINs, such as that involving OAN-e1 and MBON-e1 (Figure 10D). The latter  
595 loop potentially provides the larva with the recurrent circuits that might consolidate memories,  
596 but these are replaced by the postembryonic-born neurons that provide this function in the adult.

597       Figure 10E shows an example of a feed-forward pathway that allows the valence of a  
598 learned response to change dependent on a fly's internal state. Beyond their involvement in  
599 short-term aversive conditioning, the adult PPL1 01/MBON-11 pair functions to adjust how flies  
600 respond to a learned, aversive odor based on their hunger state (Perisse *et al.*, 2016). Amongst  
601 its other targets, MBON 11 inhibits three medial lobe MBONs (Oswald *et al.*, 2015). The  
602 activity of the latter MBONs promotes avoidance behavior while their suppression promotes  
603 approach (Oswald *et al.*, 2015; Perisse *et al.*, 2016). Neuropeptide F (dNPF) induces a hunger  
604 state in the fly; its release is elevated in hungry flies and suppressed in satiated flies. In the  
605 absence of dNPF in the satiated fly, PPL1 01 activity suppresses the inhibitory MBON 11,  
606 thereby derepressing the medial lobe MBONs and promoting avoidance behavior. In the hungry  
607 fly, dNPF release suppresses PPL1 01, resulting in elevated MBON-11 activity which suppresses  
608 the medial lobe MBONs and reduces avoidance. dNPF also enhances sugar learning in larvae  
609 (Rohwedder *et al.*, 2015). The neurons involved in the adult circuit are also present in the larva,  
610 but MBON-d1, the larval form of MBON 11, has a reduced set of MBON targets; it has  
611 moderate connections to MBON-k1 (= adult MBON 01), a weak connection to MBON-j1 (=  
612 adult MBON 02), and no connection to MBON-e2 (= adult MBON 03) (Eichler *et al.*, 2017). A  
613 more important difference from the adult circuit is that MBON-d1 is instructed by a different  
614 DAN (DAN-d1) in the larva versus the adult as described above. It is not known if DAN-d1 is a  
615 larval target for dNPF and, thereby, provides an analogous pathway for hunger state to modify  
616 learning in the larva.

617       Figure 10F shows an adult circuit involved in memory re-consolidation and extinction (see  
618 Cognigi *et al.*, 2018). PPL1 03 ( $\gamma 2\alpha'1$ ) activates the cholinergic MBON 12 (MBON- $\gamma 2\alpha'1$ )  
619 which provides feed-back excitation to PPL1 03 and also feeds across to PAM DANs that  
620 innervate the three medial lobe MBONs described above. The larva possesses the first and last  
621 cells in this circuit but lacks both the PAMs and the critical MBON 12. In its larval state, we  
622 find that PPL1 03 is DAN-d1. DAN-d1 innervates the LA compartment which has a GABAergic  
623 output through MBON-d1. This inhibitory output is ill adapted for feed-back and feed-across  
624 excitation in the larva. It is possible that this function in the larva has shifted to DAN-c1 and is  
625 associated with switch in cholinergic output from the LP compartment of the larva to the  $\gamma 2$  and  
626  $\alpha 1$  compartments of the adult. There are no direct connections from MBON-c1 back to DAN-c1  
627 (Eichler *et al.*, 2017), but the feed-forward, feed-back, and feed-across connections described by  
628 Eschbach *et al.* (2020) may provide the required pathways.

629

### 630 **The persistence of memory traces through metamorphosis.**

631       Experiments on aversive conditioning of *Drosophila* larvae suggested that the memory  
632 of larval training can endure through metamorphosis (Tully *et al.*, 1994). Our anatomical  
633 analysis did not identify any circuit elements that may support the persistence of a memory trace  
634 from larva to adult. Within the lobe system, none of the MBIN-MBON pairings persist (Figure  
635 10A) and persisting MBON to MBON connections are rare (Figure 10B). A memory trace might

636 involve more complex pathways as described by Eschbach *et al.*, 2020, but these cannot be  
637 addressed in this study.

638 Our failure to find anatomical support for persistence of a memory trace from larva to  
639 adult in *Drosophila* should not be generalized to other insects that undergo complete  
640 metamorphosis. There is compelling evidence that learning in caterpillars and beetle grubs can  
641 carry through to the adult (Blackistin *et al.*, 2008, 2015). Butterfly and beetle larvae have an  
642 extended embryonic development and hatch with a more complex nervous systems as compared  
643 to *Drosophila* larvae. The extended period of embryonic neurogenesis means that caterpillars  
644 and grubs hatch with more of the neuron types needed for constructing a functional mushroom  
645 body and, therefore, are less dependent on using trans-differentiation to generate missing neuron  
646 types. A higher incidence of the same neurons being used in the mushroom body circuits of both  
647 stages increases the likelihood that some connections persist through metamorphosis.

648

#### 649 **The evolution of a larval mushroom body.**

650 The insect metamorphic life history, which involves making different larval and adult  
651 nervous systems, arose from an ancestral condition in which the embryo generated a single  
652 nervous system that served both the nymph and the adult. In the latter, even neurons that have  
653 adult-specific functions such as those involved in flight or reproduction already have their  
654 terminal form in the hatching nymph (reviewed in Truman, 2005). Our study of the origins and  
655 fates of mushroom body neurons in *Drosophila* provides insight into how this second nervous  
656 system may have been intercalated into an ancestral plan that generated only one CNS (Figure  
657 11). Other strategies are evident in the formation of the central complex in larval beetles  
658 (Farnworth *et al.*, 2020).

659 Direct developing insects like the house cricket, *Acheta domesticus*, produce two classes  
660 of Kenyon cell classes, the  $\gamma$  and the  $\alpha\beta$  classes. Both are produced during embryogenesis with  
661 the  $\gamma$  set being made before the  $\alpha\beta$  cells (Malaterre *et al.*, 2002). With the exception of the optic  
662 lobes (Anderson, 1978) and the addition of more  $\alpha\beta$  Kenyon cells (Malaterre *et al.*, 2002), direct  
663 developing insects finish producing neurons for their CNS during embryogenesis (Shepherd &  
664 Bate, 1990; Truman & Ball, 1998). Consequently, all of their mushroom body extrinsic neurons  
665 should be present at hatching, and we assume that the relative times of their birth mirrors that of  
666 their Kenyon cell targets. In other words, we assume that the MBONs and MBINs innervating  
667 the  $\gamma$  cells are born before those innervating the  $\alpha\beta$  neurons, and that both sets are present in the  
668 first stage nymph. Unfortunately, though, the temporal sequence by which these cells arise has  
669 not yet been determined for any direct developing insect.

670 Compared to their direct developing relatives, *Drosophila* embryos undergo an early  
671 arrest in neurogenesis, resulting in a larval brain that contains about 10% of the neurons found in  
672 the adult central brain. We find that this truncation results in the presence of  $\gamma$  neurons and many  
673 of the early-born extrinsic neurons that innervate them, but the later-born  $\alpha\beta$  Kenyon cells and  
674 their input and output neurons are absent. The terminal fates of these earliest-born neurons are  
675 for the medial lobe and many are used as such for the larva, but making a vertical lobe is a

676 problem because of the lack of  $\alpha\beta$  and  $\alpha'\beta'$  Kenyon cells and their extrinsic neurons. We find  
677 that the larva solves this problem by constructing a “facsimile” of a vertical lobe. This involves  
678 modifying the  $\gamma$  Kenyon cells with a larval-specific vertical axon branch to form the core of the  
679 vertical lobe facsimile and finding substitutes for the missing vertical lobe MBINs and MBONs.  
680 The latter were recruited from early-born neurons that were destined for adult circuits not needed  
681 in the larva or from “spare” medial lobe MBONs that are redirected to the vertical lobe. These  
682 neurons assume a temporary identity that is maintained through larval life but, when the larval  
683 vertical lobe facsimile is disassembled at metamorphosis, they trans-differentiate to assume their  
684 terminal identity in the adult brain. As the larval system is being disassembled, the  $\alpha\beta$  and  $\alpha'\beta'$   
685 neurons and their late-born extrinsic cells then construct the adult vertical lobes. Consequently,  
686 from the perspective of the adult, the relative temporal ordering of the production of the Kenyon  
687 cell types and their corresponding MBINs and MBONs remains the same as is thought to exist in  
688 the direct developing insects from which they evolved.

689 The ability of some neurons to trans-differentiate and thereby perform different functions  
690 in the larva versus the adult seems crucial for making a sophisticated larval CNS. Our  
691 observations on the metamorphic fates of the lineage 13B leg interneurons (Figure 6) argue that  
692 the adult identities of these neurons are their ancestral identities, and their assumed, larval  
693 identities are a derived condition supporting the evolution of a larva. A seminal paper by  
694 Thomas *et al.* (1984) indicated that the neuron types for the insect CNS are generated according  
695 to a set of highly conserved spatial and temporal rules that have changed little through the span  
696 of insect evolution. Our findings for the adult mushroom bodies are consistent with this notion,  
697 but the production of some cell types for the larval system, such as the early appearance of  
698 MBINs and MBONs for the larva vertical lobe, appear to break these rules. While the assumed  
699 identity and function of these neurons in the larva appear to deviate from the ancestral plan for  
700 making neuron types, we find that their terminal identities are in accord with it. In other words,  
701 the ability of some neurons to trans-differentiate allows them to both maintain the rules for  
702 generating neuronal phenotypes for the adult while also temporarily suspending or modifying  
703 such rules to generate an assumed identity for these cells while in the larva. Trans-  
704 differentiation allowed these neurons to uncouple their larval functions from those of the adult,  
705 thereby allowing selection to potentially modify one version of the cell without impacting the  
706 other. The evolutionary success of insects with complete metamorphosis is attributed to the  
707 larval and adult stages being based on independent developmental modules that allow selection  
708 to change one without compromising the other [Yang, 2001]. Trans-differentiating neurons  
709 provide a cellular example of such an uncoupling. We do not yet know how these neurons  
710 achieve an uncoupling that allows them to assume two different identities during the life of the  
711 animal, although, as speculated above, we expect that temporary changes may occur within  
712 lineages to alter the temporal or spatial information that direct neuronal identity. Besides  
713 providing insight into a key innovation in insect evolution, understanding natural mechanisms by  
714 which cell fates are changed in insects may reveal new mechanisms that will be useful in  
715 changing neuronal phenotypes in other animals to deal with issues in aging or disease.

716

## 717 Materials & Methods

### 718 Fly stocks

719 Drosophila stocks were raised on standard corn meal-molasses at either 25°C or room  
720 temperature. The genetic stocks used in this study are summarized in Tables 4 and 5.

721

### 722 Flp-Switch treatments

723 The expression pattern seen in the late 3<sup>rd</sup> instar in stable spilt lines was maintained  
724 through metamorphosis using the Flip-Switch method described in Harris *et al.* (2015). Using a  
725 similar strategy of the gene-switch method (Roman *et al.*, 2001), flippase was fused to the  
726 ligand-binding domain of the human progesterone receptor, rendering it dependent on  
727 progesterone or a progesterone mimic to move into the nucleus. Stable spilt lines were crossed  
728 to *pJFRC48-13XLexAop2-IVS-myrtdTomo in su(Hw)attP8; Actin5Cp4.6>dsFRT>LexAp65 in*  
729 *su(Hw)attP5; pJFRC108-20XUAS-IVS-hPRFlp-p10 in VK00005/TM6*.

730 We used the progesterone mimic mifepristone (RU486, Sigma Aldrich; #M8046) to  
731 cause translocation of the flippase to the nucleus where it could then flip-out the STOP cassette  
732 in the Actin-LexAp65 transgene. We used surface application of RU486 to food vials. Parents  
733 were allowed to lay eggs in a food vial for a few days, then transferred to a fresh vial.  
734 Approximately 4 days after transfer, 60µl of a ~10mM RU486 stock solution (10 mg RU486  
735 dissolved in 2 ml 95% ethanol) was applied to the surface of the food. At 24 h after treatment,  
736 any larvae that had wandered and/or pupariated were discarded to ensure that test animals had  
737 fed on RU486 for at least 24 h. At 48h after treatment, the subsequent wandering larvae and  
738 pupae (which had all fed on RU486 for 24-48 h during the L3 stage) were collected and  
739 transferred to an untreated food vial. These animals were then dissected in Schneider's S2  
740 culture medium as adults. This treatment results in constitutive LexA expression in any cells that  
741 express GAL4 during the L3 stage, but, because the RU486 persists at least partway through  
742 metamorphosis neurons that start expressing in early to mid-metamorphosis also show up.  
743 .

### 744 Lineage-targeted twin-spot MARCM

745 Specific neuronal lineages were targeted using lineage-restricted drivers (Awasaki *et al.*,  
746 2014) to label sister clones with twin-spot MARCM (Yu *et al.*, 2009). The Vnd-GAL4 driver  
747 permits targeting 18 fly central brain lineages, including the FLAa2 lineage (Lee *et al.*, 2020);  
748 and stg14-GAL4 driver covers eight type II neuronal lineages, including the DL1  
749 lineage (Wang *et al.*, 2014). Twin-spot clones were induced at specific times after larval  
750 hatching and examined at the adult stage by immunostaining and confocal imagining, following  
751 published work (e.g. Yu *et al.*, 2010).

752

### 753 Preparation and examination of tissues

754 Tissues were dissected in PBS (phosphate-buffered saline, pH 7.8) and fixed in 4%  
755 buffered formaldehyde overnight at 4°C. Fixed tissues were rinsed in PBS-TX (PBS with 1%  
756 Triton X-100, Sigma), then incubated overnight at 4°C in a cocktail of 10% normal donkey

757 serum (Jackson ImmunoResearch), 1:1000 rabbit anti-GFP (Jackson ImmunoResearch), 1:40 rat  
758 anti-N-Cadherin (Developmental Studies Hybridoma Bank), and 1:40 mouse anti-Neuroglan or  
759 a 1:200 dilution of mouse anti-FasII (both Developmental Studies Hybridoma Bank). For  
760 visualization of tdTomato, a 1:500 dilution of rabbit anti-DsRed (CloneTech) was substituted for  
761 the anti-GFP and the anti-Neuroglan was omitted. After repeated rinses PBS-TX, tissues  
762 stained for GFP were incubated overnight at 4°C with 1:500 AlexaFluor 488-conjugated donkey  
763 anti-rabbit, AlexaFluor 594-conjugated donkey anti-mouse, and AlexaFluor 649-conjugated  
764 donkey anti-rat (all from Invitrogen). For visualization of RFP staining was with a 1:500 dilution  
765 of AlexaFluor 594-conjugated donkey anti-rabbit and AlexaFluor 649-conjugated donkey anti-  
766 rat. After exposure to secondaries, tissues were then washed in PBS-TX, mounted onto poly-  
767 Lysine-coated coverslips, dehydrated through an ethanol series, cleared in xylenes, and mounted  
768 in DPX mountant (Sigma-Aldrich). Nervous systems were imaged on a Zeiss LSM 510 confocal  
769 microscope at 40x with optical sections taken at 2µm intervals. LSM files were contrast-  
770 enhanced as necessary and z-projected using ImageJ (<http://rsbweb.nih.gov/ij/>). Reagents  
771 summarized in Table 6.

772

### 773 **Acknowledgements**

774

775 We are grateful to Scarlett Pitts and Todd Laverty of the Janelia FlyCore for dealing with  
776 *Drosophila* maintenance and setting up the needed crosses. Members of the Janelia FlyLight  
777 team including Geoffrey Meissner, Susana Tae, Jennifer Jeter, Scott Miller and Sophia  
778 Protopapas were involved in dissection, immunocytochemistry, and imaging. We thank Lynn  
779 Riddiford for critical comments on the manuscript. The research was funded by HHMI.

780

### 781 **Competing Interests:**

782

783 The authors have no competing interests.

784

### 785 **References**

786

787 Anderson, H. (1978). Postembryonic development of the visual system of the locust,  
788 *Schistocerca gregaria*. I. Patterns of growth and developmental interactions in the retina  
789 and optic lobe. *J. Emb. Exp. Morph.* **45**: 55–83.

790 Armstrong, J. D., J. S. de Belle, Z. Wang, and K. Kaiser. (1998). Metamorphosis of the  
791 mushroom bodies; large-scale rearrangements of the neural substrates for associative  
792 learning and memory in *Drosophila*. *Learn. Mem.* **5**:102-114.

793 Aso, Y., Hattori, D., Yu, Y., Johnston, R. M., Iyer, N. A., Ngo, T. T., Dionne, H., Abbott, L. F.,  
794 Axel, R., Tanimoto, H., & Rubin, G. M. (2014). The neuronal architecture of the mushroom  
795 body provides a logic for associative learning. *eLife* **3**, e04577. doi.org/10.7554/eLife.04577

796 Aso, Y., Herb, A., Ogueta, M., Siwanowicz, I., Templier, T., Friedrich, A. B., Ito, K., Scholz, H.,  
797 & Tanimoto, H. (2012). Three dopamine pathways induce aversive odor memories with  
798 different stability. *PLoS genetics* **8**: e1002768. doi.org/10.1371/journal.pgen.1002768

799 Awasaki, T., Kao, C. F., Lee, Y. J., Yang, C. P., Huang, Y., Pfeiffer, B. D., Luan, H., Jing, X.,  
800 Huang, Y. F., He, Y., Schroeder, M. D., Kuzin, A., Brody, T., Zugates, C. T., Odenwald, W.  
801 F., & Lee, T. (2014). Making *Drosophila* lineage-restricted drivers via patterned  
802 recombination in neuroblasts. *Nature Neurosci* **17**: 631–637. doi.org/10.1038/nn.3654

803 Awasaki, T., & Ito, K. (2004). Engulfing action of glial cells is required for programmed axon  
804 pruning during *Drosophila* metamorphosis. *Curr. Biol.* **14**: 668–677.  
805 doi.org/10.1016/j.cub.2004.04.001

806 Blackiston, D. J., Shomrat, T., & Levin, M. (2015). The stability of memories during brain  
807 remodeling: A perspective. *Commun. & Integrative Biol.* **8**: e1073424.  
808 doi.org/10.1080/19420889.2015.1073424

809 Blackiston, D. J., Silva Casey, E., & Weiss, M. R. (2008). Retention of memory through  
810 metamorphosis: can a moth remember what it learned as a caterpillar?. *PLoS One* **3**: e1736.  
811 doi.org/10.1371/journal.pone.0001736

812 Boone, J. Q., & Doe, C. Q. (2008). Identification of *Drosophila* type II neuroblast lineages  
813 containing transit amplifying ganglion mother cells. *Dev. Neurobiol.* **68**: 1185–1195.  
814 doi.org/10.1002/dneu.20648

815 Busch, S., Selcho, M., Ito, K., & Tanimoto, H. (2009). A map of octopaminergic neurons in the  
816 *Drosophila* brain. *J. Comp. Neurol.* **513**: 643–667. doi.org/10.1002/cne.21966.

817 Busch, S., & Tanimoto, H. (2010). Cellular configuration of single octopamine neurons in  
818 *Drosophila*. *J. Comp. Neurol.* **518**: 2355–2364. doi.org/10.1002/cne.22337

819 Cognigni, P., Felsenberg, J., & Waddell, S. (2018). Do the right thing: neural network  
820 mechanisms of memory formation, expression and update in *Drosophila*. *Curr. Opinion  
821 Neurobiol.* **49**: 51–58. doi.org/10.1016/j.conb.2017.12.002

822 Consoulas, C., Restifo, L. L., & Levine, R. B. (2002). Dendritic remodeling and growth of  
823 motoneurons during metamorphosis of *Drosophila melanogaster*. *J. Neurosci.* **22**: 4906–  
824 4917. doi.org/10.1523/JNEUROSCI.22-12-04906.2002

825 Das, G., Klappenbach, M., Vrontou, E., Perisse, E., Clark, C. M., Burke, C. J., & Waddell, S.  
826 (2014). *Drosophila* learn opposing components of a compound food stimulus. *Curr. Biol.* **24**:  
827 1723–1730. doi.org/10.1016/j.cub.2014.05.078

828 Doe C. Q. (2017). Temporal Patterning in the *Drosophila* CNS. *Ann. Rev. Cell Dev. Biol.* **33**:  
829 219–240. doi.org/10.1146/annurev-cellbio-111315-125210

830 Dolan, M.-J., S. Frechter, A.S.Bates, C. Dan, P. Huoviala, R.J.V.Roberts, P. Schlegel, S.  
831 Dhawan, R. Tabano, H. Dionne, C. Christoforou, K. Close, B. Sutcliffe, B. Giuliani, F. Li,  
832 M. Costa, G. Ihrke, G.W.Meissner, D.D.Bodk, Y. Aso, G.M.Rubin, G.S.X.E.Jefferis. (2019)  
833 Neurogenetic dissection of the *Drosophila* lateral horn reveals major outputs, diverse  
834 behavioral functions, and interactions with the mushroom body. *eLife* **8**:e43079 doi:  
835 10.7554/eLife.43079.001

836 Eichler, K., Li, F., Litwin-Kumar, A., Park, Y., Andrade, I., Schneider-Mizell, C. M.,  
837 Saumweber, T., Huser, A., Eschbach, C., Gerber, B., Fetter, R. D., Truman, J. W., Priebe, C.

838 E., Abbott, L. F., Thum, A. S., Zlatic, M., & Cardona, A. (2017). The complete connectome  
839 of a learning and memory centre in an insect brain. *Nature* **548**: 175–182.  
840 doi.org/10.1038/nature23455

841 Eschbach, C., Fushiki, A., Winding, M., Schneider-Mizell, C. M., Shao, M., Arruda, R., Eichler,  
842 K., Valdes-Aleman, J., Ohyama, T., Thum, A. S., Gerber, B., Fetter, R. D., Truman, J. W.,  
843 Litwin-Kumar, A., Cardona, A., & Zlatic, M. (2020). Recurrent architecture for adaptive  
844 regulation of learning in the insect brain. *Nat. Neurosci* **23**: 544–555.  
845 doi.org/10.1038/s41593-020-0607-9

846 Farnworth, M. S., Eckermann, K. N., & Bucher, G. (2020). Sequence heterochrony led to a gain  
847 of functionality in an immature stage of the central complex: A fly-beetle insight. *PLoS  
848 Biol.* **18**, e3000881. doi.org/10.1371/journal.pbio.3000881

849 Farris, S. M., & Sinakevitch, I. (2003). Development and evolution of the insect mushroom  
850 bodies: towards the understanding of conserved developmental mechanisms in a higher brain  
851 center. *Arthropod Struc. Dev.* **32**: 79–101. doi.org/10.1016/S1467-8039(03)00009-4

852 Harris, R. M., Pfeiffer, B. D., Rubin, G. M., & Truman, J. W. (2015). Neuron hemilineages  
853 provide the functional ground plan for the *Drosophila* ventral nervous system. *eLife*, **4**:  
854 e04493. doi.org/10.7554/eLife.04493

855 Hobert, O., & Kratsios, P. (2019). Neuronal identity control by terminal selectors in worms, flies,  
856 and chordates. *Curr. Opinion Neurobiol.* **56**: 97–105. doi.org/10.1016/j.conb.2018.12.006

857 Ichinose, T., Aso, Y., Yamagata, N., Abe, A., Rubin, G.M., & Tanimoto, H. (2015). Reward  
858 signal in a recurrent circuit drives appetitive long-term memory formation. *eLife* **4**: e10719.  
859 doi: 10.7554/eLife.10719.

860 Jacobs, J. R., & Goodman, C. S. (1989). Embryonic development of axon pathways in the  
861 *Drosophila* CNS. II. Behavior of pioneer growth cones. *J. Neurosci.* **9**: 2412–2422.  
862 doi.org/10.1523/JNEUROSCI.09-07-02412.1989

863 Kanold, P. O., Kara, P., Reid, R. C., & Shatz, C. J. (2003). Role of subplate neurons in functional  
864 maturation of visual cortical columns. *Science* **301**: 521–525.  
865 doi.org/10.1126/science.1084152

866 Kohwi, M. and Doe, C. Q. (2013) Temporal fate specification and neural progenitor competence  
867 during development. *Nature Rev. Neurosci.* **14**: 823-838.

868 Lacin, H., and J. W. Truman, 2016 Lineage mapping identifies molecular and architectural  
869 similarities between the larval and adult *Drosophila* central nervous system. *eLife* **5**: e13399.

870 Lee, K., & Doe, C. Q. (2021). A locomotor neural circuit persists and functions similarly in  
871 larvae and adult *Drosophila*. *eLife*, **10**: e69767. doi.org/10.7554/eLife.69767

872 Lee, T., Lee, A., & Luo, L. (1999). Development of the *Drosophila* mushroom bodies: sequential  
873 generation of three distinct types of neurons from a neuroblast. *Development* **126**: 4065–  
874 4076.

875 Lee, T., Marticke, S., Sung, C., Robinow, S., & Luo, L. (2000). Cell-autonomous requirement of  
876 the USP/EcR-B ecdysone receptor for mushroom body neuronal remodeling in  
877 *Drosophila*. *Neuron* **28**: 807–818. doi.org/10.1016/s0896-6273(00)00155-0

878 Lee, Y. J., Yang, C. P., Miyares, R. L., Huang, Y. F., He, Y., Ren, Q., Chen, H. M., Kawase, T.,  
879 Ito, M., Otsuna, H., Sugino, K., Aso, Y., Ito, K., & Lee, T. (2020). Conservation and

880 divergence of related neuronal lineages in the *Drosophila* central brain. *eLife*, **9**: e53518.  
881 doi.org/10.7554/eLife.53518

882 Levine, R. B., & Truman, J. W. (1985). Dendritic reorganization of abdominal motoneurons  
883 during metamorphosis of the moth, *Manduca sexta*. *J. Neurosci.* **5**: 2424–2431.  
884 doi.org/10.1523/JNEUROSCI.05-09-02424.1985

885 Li, F., Lindsey, J. W., Marin, E. C., Otto, N., Dreher, M., Dempsey, G., Stark, I., Bates, A. S.,  
886 Pleijzier, M. W., Schlegel, P., Nern, A., Takemura, S. Y., Eckstein, N., Yang, T., Francis, A.,  
887 Braun, A., Parekh, R., Costa, M., Scheffer, L. K., Aso, Y., ... Rubin, G. M. (2020). The  
888 connectome of the adult *Drosophila* mushroom body provides insights into function. *eLife*, **9**:  
889 e62576. doi.org/10.7554/eLife.62576

890 Li, H., Shuster, S. A., Li, J., & Luo, L. (2018). Linking neuronal lineage and wiring  
891 specificity. *Neur. Dev.* **13**: 5. doi.org/10.1186/s13064-018-0102-0

892 Malaterre, J., Strambi, C., Chiang, A. S., Aouane, A., Strambi, A., & Cayre, M. (2002).  
893 Development of cricket mushroom bodies. *J. Comp. Neurol.* **452**: 215–227.  
894 doi.org/10.1002/cne.10319

895 Mao, Z., & Davis, R. L. (2009). Eight different types of dopaminergic neurons innervate the  
896 *Drosophila* mushroom body neuropil: anatomical and physiological heterogeneity. *Front.*  
897 *Neur. Circuits* **3**: 5. doi.org/10.3389/neuro.04.005.2009

898 Mayseless, O., D.S.Berns, X.M.Yu, T. Riemensperger, A.Fiala, & O.Schuldiner (2018)  
899 Developmental coordination during olfactory circuit remodeling in *Drosophila*. *Neuron*  
900 **99**:1204-1215.

901 Miyares, R. L., & Lee, T. (2019). Temporal control of *Drosophila* central nervous system  
902 development. *Curr. Opinion Neurobiol.* **56**: 24–32. doi.org/10.1016/j.conb.2018.10.016.

903 Monastirioti, M., Giagtzoglou, N., Koumbanakis, K. A., Zacharioudaki, E., Deligiannaki, M.,  
904 Wech, I., Almeida, M., Preiss, A., Bray, S., & Delidakis, C. (2010). *Drosophila Hey* is a  
905 target of Notch in asymmetric divisions during embryonic and larval  
906 neurogenesis. *Development* **137**: 191–201. doi.org/10.1242/dev.043604

907 Ren, Q., Awasaki, T., Huang, Y. F., Liu, Z., & Lee, T. (2016). Cell Class-Lineage Analysis  
908 Reveals Sexually Dimorphic Lineage Compositions in the *Drosophila* Brain. *Curr. Biol.* **26**:  
909 2583–2593. doi.org/10.1016/j.cub.2016.07.086

910 Rohwedder, A., Selcho, M., Chassot, B., & Thum, A. S. (2015). Neuropeptide F neurons  
911 modulate sugar reward during associative olfactory learning of *Drosophila* larvae. *J. Comp.*  
912 *Neuro.* **523**: 2637–2664. doi.org/10.1002/cne.23873

913 Roman, G., Endo, K., Zong, L., & Davis, R. L. (2001). P[Switch], a system for spatial and  
914 temporal control of gene expression in *Drosophila melanogaster*. *Proc. Natl. Acad. Sci.*  
915 (USA) **98**: 12602–12607. doi.org/10.1073/pnas.221303998

916 Rossi, A. M., Jafari, S., & Desplan, C. (2021). Integrated Patterning Programs  
917 During *Drosophila* Development Generate the Diversity of Neurons and Control Their  
918 Mature Properties. *Ann. Rev. Neurosci.* **44**: 153-172. doi.org/10.1146/annurev-neuro-102120-  
919 014813

920 Roy, B., Singh, A. P., Shetty, C., Chaudhary, V., North, A., Landgraf, M., Vijayraghavan, K., &  
921 Rodrigues, V. (2007). Metamorphosis of an identified serotonergic neuron in the *Drosophila*  
922 olfactory system. *Neural Dev.* **2**: 20. doi.org/10.1186/1749-8104-2-20

923 Saumweber, T., Rohwedder, A., Schleyer, M., Eichler, K., Chen, Y. C., Aso, Y., Cardona, A.,  
924 Eschbach, C., Kobler, O., Voigt, A., Durairaja, A., Mancini, N., Zlatic, M., Truman, J. W.,  
925 Thum, A. S., & Gerber, B. (2018). Functional architecture of reward learning in mushroom  
926 body extrinsic neurons of larval *Drosophila*. *Nature Comm.* **9**: 1104.  
927 doi.org/10.1038/s41467-018-03130-1

928 Schubiger, M., Wade, A. A., Carney, G. E., Truman, J. W., & Bender, M. (1998). *Drosophila*  
929 EcR-B ecdysone receptor isoforms are required for larval molting and for neuron  
930 remodeling during metamorphosis. *Development* **125**: 2053–2062.  
931 doi.org/10.1242/dev.125.11.2053

932 Selcho, M., Pauls, D., Han, K. A., Stocker, R. F., & Thum, A. S. (2009). The role of dopamine in  
933 *Drosophila* larval classical olfactory conditioning. *PloS one*, **4**: e5897.  
934 doi.org/10.1371/journal.pone.0005897

935 Siegler, M. V., & Burrows, M. (1984). The morphology of two groups of spiking local  
936 interneurons in the metathoracic ganglion of the locust. *J. Comp. Neurol.* **224**: 463–482.  
937 doi.org/10.1002/cne.902240402

938 Shepherd, D., & Bate, C.M. (1990). Spatial and temporal patterns of neurogenesis in the embryo  
939 of the locust (*Schistocerca gregaria*). *Development* **108**, 83-96.

940 Shepherd, D., & Laurent, G. (1992). Embryonic development of a population of spiking local  
941 interneurons in the locust (*Schistocerca gregaria*). *J. Comp. Neurol.* **319**: 438–453.  
942 doi.org/10.1002/cne.903190309

943 Skeath, J. B., & Doe, C. Q. (1998). Sanpodo and Notch act in opposition to Numb to distinguish  
944 sibling neuron fates in the *Drosophila* CNS. *Development* **125**: 1857–1865.  
945 doi.org/10.1242/dev.125.10.1857

946 Taghert, P. H., & Goodman, C. S. (1984). Cell determination and differentiation of identified  
947 serotonin-immunoreactive neurons in the grasshopper embryo. *J. Neurosci.* **4**: 989–1000.  
948 doi.org/10.1523/JNEUROSCI.04-04-00989.1984

949 Tanaka, N. K., Tanimoto, H., & Ito, K. (2008). Neuronal assemblies of the *Drosophila*  
950 mushroom body. *J. Comp. Neurol.* **508**: 711–755. doi.org/10.1002/cne.21692

951 Technau, G., and M. Heisenberg. (1982) Neural reorganization during metamorphosis of the  
952 corpora pedunculata in *Drosophila melanogaster*. *Nature* **295**: 405-407.

953 Thomas, J. B., Bastiani, M. J., Bate, M., & Goodman, C. S. (1984). From grasshopper to  
954 *Drosophila*: a common plan for neuronal development. *Nature* **310** 203–207.  
955 doi.org/10.1038/310203a0

956 Thompson, K. J., & Siegler, M. V. (1993). Development of segment specificity in identified  
957 lineages of the grasshopper CNS. *J. Neurosci.* **13**: 3309–3318.  
958 doi.org/10.1523/JNEUROSCI.13-08-03309.1993

959 Thum, A. S., & Gerber, B. (2019). Connectomics and function of a memory network: the  
960 mushroom body of larval *Drosophila*. *Curr. Opin. Neurobiol.* **54**: 146–154.  
961 doi.org/10.1016/j.conb.2018.10.007

962 Truman, J. W. (2005) Hormonal control of the form and function of the nervous system. In:  
963 *Comprehensive Molecular Insect Science* (L. I. Gilbert, K. Iatrou, S. S. Gill, eds.), Vol 2, pp.  
964 135-163. Elsevier, Amsterdam.

965 Truman, J. W., & Reiss, S. E. (1976). Dendritic reorganization of an identified motoneuron  
966 during metamorphosis of the tobacco hornworm moth. *Science*, **192**: 477–479.  
967 doi.org/10.1126/science.1257782

968 Truman, J. W., & Ball, E. E. (1998). Patterns of embryonic neurogenesis in a primitive wingless  
969 insect, the silverfish, *Ctenolepisma longicaudata*: comparison with those seen in flying  
970 insects. *Dev. Genes Evol.* **208**: 357–368. doi.org/10.1007/s004270050192

971 Tsuji, T., Hasegawa, E., & Isshiki, T. (2008). Neuroblast entry into quiescence is regulated  
972 intrinsically by the combination of spatial hox proteins and temporal identity factors.  
973 *Development* **135**: 3859-3869.

974 Tully, T., Cambiazo, V., & Kruse, L. (1994). Memory through metamorphosis in normal and  
975 mutant *Drosophila*. *J. Neurosci.* **14**: 68–74. doi.org/10.1523/JNEUROSCI.14-01-00068.1994

976 Urbach, R., & Technau, G. M. (2003). Early steps in building the insect brain: neuroblast  
977 formation and segmental patterning in the developing brain of different insect  
978 species. *Arthropod Struc. & Dev.* **32**: 103–123. doi.org/10.1016/S1467-8039(03)00042-2

979 Veverysa, L., & Allan, D. W. (2013). Subtype-specific neuronal remodeling during *Drosophila*  
980 metamorphosis. *Fly* **7**: 78–86. doi.org/10.4161/fly.23969

981 Watts, R. J., Hoopfer, E. D., & Luo, L. (2003). Axon pruning during *Drosophila* metamorphosis:  
982 evidence for local degeneration and requirement of the ubiquitin-proteasome  
983 system. *Neuron* **38**: 871–885. doi.org/10.1016/s0896-6273(03)00295-2

984 Witten, J. L., & Truman, J. W. (1998). Distribution of GABA-like immunoreactive neurons in  
985 insects suggests lineage homology. *J. Comp. Neurol.* **398**: 515–528.  
986 doi.org/10.1002/(sici)1096-9861(19980907)398:4<515::aid-cne4>3.0.co;2-5

987 Wright MA, Mo W, Nicolson T, Ribera AB. (2010) In vivo evidence for transdifferentiation of  
988 peripheral neurons. *Development* **137**:3047-3056. dx.doi.org/10.1242/dev.052696;  
989 PMID: 20685733

990 Wolff, T. & and G.M.Rubin. G. M. (2018). Neuroarchitecture of the *Drosophila* central complex:  
991 A catalog of nodulus and asymmetrical body neurons and a revision of the protocerebral  
992 bridge catalog. *J. Comp. Neurol.* **526**: 2585-2611.

993 Yang A. S. (2001). Modularity, evolvability, and adaptive radiations: a comparison of the hemi-  
994 and holometabolous insects. *Evol. Dev.* **3**: 59–72. doi.org/10.1046/j.1525-  
995 142x.2001.003002059.x

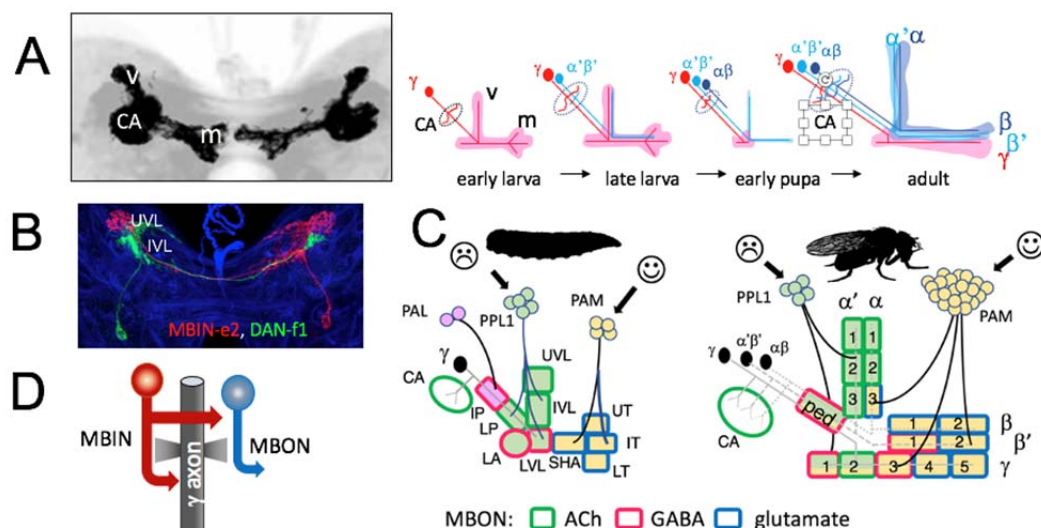
996 Wang, Y. C., Yang, J. S., Johnston, R., Ren, Q., Lee, Y. J., Luan, H., Brody, T., Odenwald, W.  
997 F., & Lee, T. (2014). *Drosophila* intermediate neural progenitors produce lineage-dependent  
998 related series of diverse neurons. *Development* **141**: 253–258.

999 Williams, D. W., & Truman, J. W. (2005). Cellular mechanisms of dendrite pruning in  
1000 *Drosophila*: insights from in vivo time-lapse of remodeling dendritic arborizing sensory  
1001 neurons. *Development* **132**: 3631–3642. https://doi.org/10.1242/dev.01928

1002 Yaniv, S. P., Issman-Zecharya, N., Oren-Suissa, M., Podbilewicz, B., & Schuldiner, O. (2012).  
1003 Axon regrowth during development and regeneration following injury share molecular  
1004 mechanisms. *Curr. Biol.* **22**: 1774–1782. <https://doi.org/10.1016/j.cub.2012.07.044>  
1005 Yu, H. H., Chen, C. H., Shi, L., Huang, Y., & Lee, T. (2009). Twin-spot MARCM to reveal the  
1006 developmental origin and identity of neurons. *Nature Neurosci.* **12**: 947–953.  
1007 [doi.org/10.1038/nn.2345](https://doi.org/10.1038/nn.2345)  
1008 Yu, H. H., Kao, C. F., He, Y., Ding, P., Kao, J. C., & Lee, T. (2010). A complete developmental  
1009 sequence of a Drosophila neuronal lineage as revealed by twin-spot MARCM. *PLoS Biol.* **8**:  
1010 e1000461. <https://doi.org/10.1371/journal.pbio.1000461>  
1011 Zheng, Z., Lauritzen, J. S., Perlman, E., Robinson, C. G., Nichols, M., Milkie, D., Torrens, O.,  
1012 Price, J., Fisher, C. B., Sharifi, N., Calle-Schuler, S. A., Kmecova, L., Ali, I. J., Karsh, B.,  
1013 Trautman, E. T., Bogovic, J. A., Hanslovsky, P., Jefferis, G., Kazhdan, M., Khairy, K., ...  
1014 Bock, D. D. (2018). A Complete Electron Microscopy Volume of the Brain of Adult  
1015 Drosophila melanogaster. *Cell* **174**: 730–743.e22. [doi.org/10.1016/j.cell.2018.06.019](https://doi.org/10.1016/j.cell.2018.06.019)  
1016

1017  
1018  
1019  
1020  
1021  
1022

1023 **Figure 1**



1024  
1025 **Figure 1.** The organization of the larval and adult mushroom bodies in the *Drosophila* brain. **A.** Structure and  
1026 development of the intrinsic cells (Kenyon cells) of the mushroom body through larval life and  
1027 metamorphosis. The confocal projection shows a larval brain with the paired mushroom bodies; dendrites  
1028 project to the calyx (CA) and the axons bifurcate into the vertical (v) and medial (m) lobes. Schematic shows  
1029 the anatomy of the  $\gamma$  Kenyon cells found in the larva; these are later joined by  $\alpha'\beta'$  and  $\alpha\beta$  Kenyon cells to  
1030 form the medial ( $\gamma$ ,  $\beta'$ ,  $\beta$ ) and vertical ( $\alpha'$ ,  $\alpha$ ) lobe systems of the adult. **B.** Projection of a multicolor flip-  
1031 out (MCFO) image from larval brain showing two mushroom body input neurons that project bilaterally  
1032 to the upper (UVL) and intermediate (IVL) compartments of the vertical lobes. **C.** The mushroom body  
1033 peduncle (ped) and lobe systems are divided into computational compartments defined by the  
1034 projections from three clusters of aminergic neurons, the PAL (light red), PPL1 (light green) and PAM  
1035 (yellow) clusters. PPL1 input largely indicates punishment, and PAM input indicates reward. These  
1036 interact with Kenyon cell axons and mushroom body output neurons (MBONs) to cause either avoidance  
1037 or attraction. The MBON transmitter is indicated by the outline of each compartment. The adult has 16  
1038 compartments compared to the ten compartments of the larva. Larval compartments: CA: calyx; IP and  
1039 LP: intermediate and lower peduncle; LA: lateral appendix; UVL, IVL, LVL: upper, intermediate and  
1040 lower vertical lobe; SHA: shaft; UT, IT, LT: upper, intermediate and lower toe. **D.** Schematic of the  
1041 microcircuitry of larval and adult compartments.  
1042

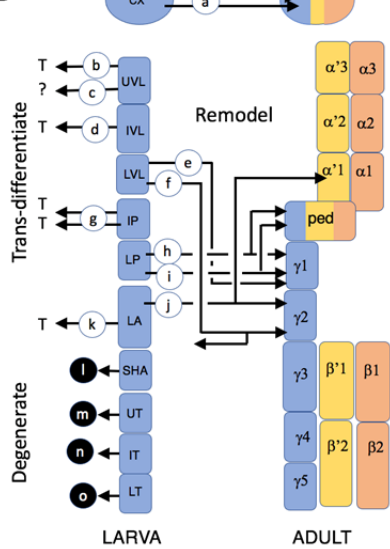
1043  
1044

1045 **Figure 2**

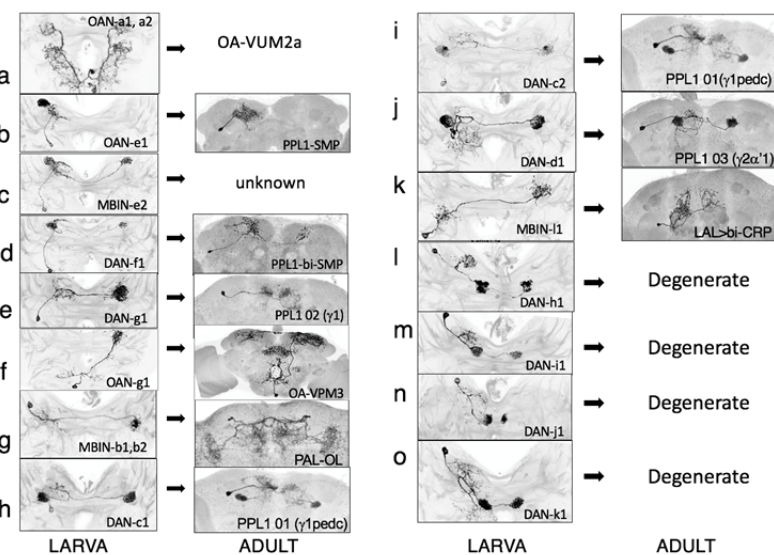
**A**



**B**



**C**

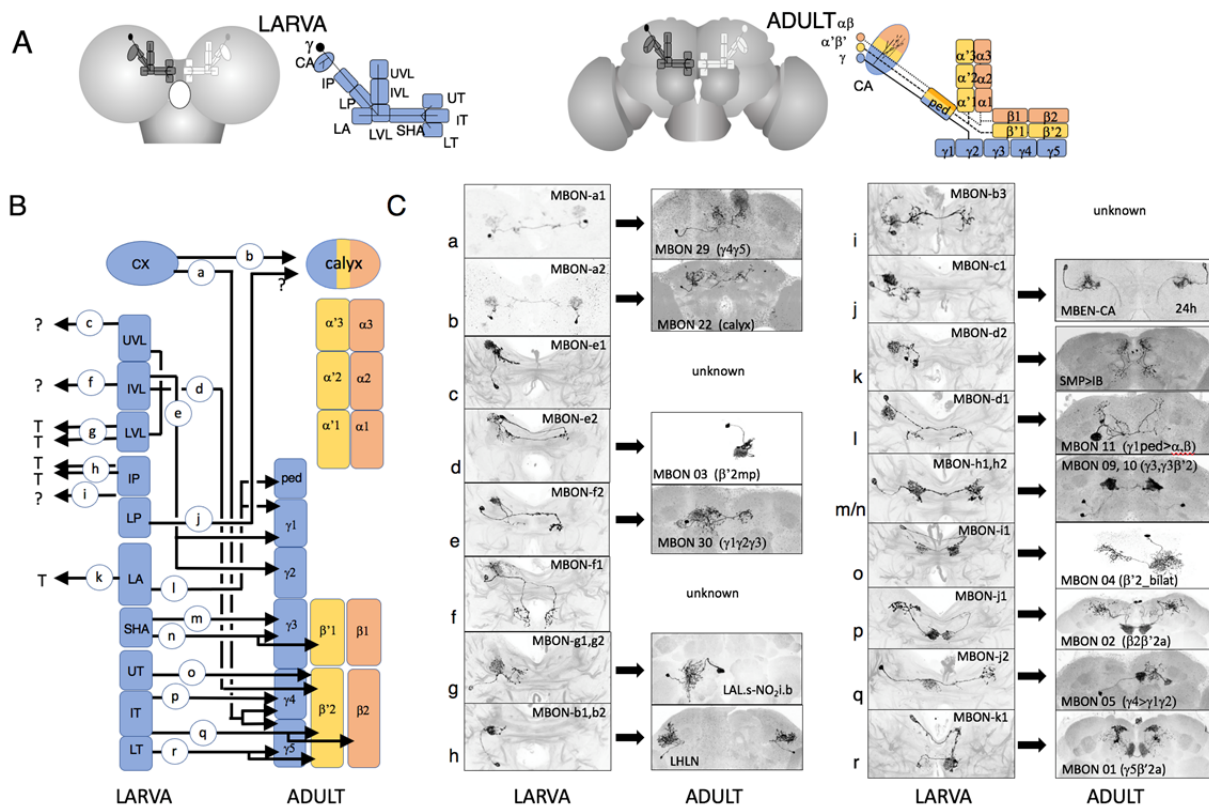


1046  
1047

1048 **Figure 2. The metamorphic fates of the larval mushroom body input cells (MBINs). (A)**

1049 Comparison of compartment structure of the larval and adult brain. Compartment color indicates the  
1050 Kenyon cell axons each possesses. Compartment names as in Fig 1. **(B)** Schematic summarizing the  
1051 fates of the compartmental MBINs of the larva. Arrows indicate whether cells remodel and remain as  
1052 MBINs, trans-differentiate to have different functions in the adult, or degenerate. Lower case letters  
1053 refer to images in part C. **(C)** Images comparing the larval and adult forms of the larval MBINs based on  
1054 flip-switch immortalization. The images and names of the larval cells from Saumweber *et al.* 2018; adult  
1055 names based on Aso *et al.*, 2014 and Li *et al.*, 2020, or this study  
1056  
1057

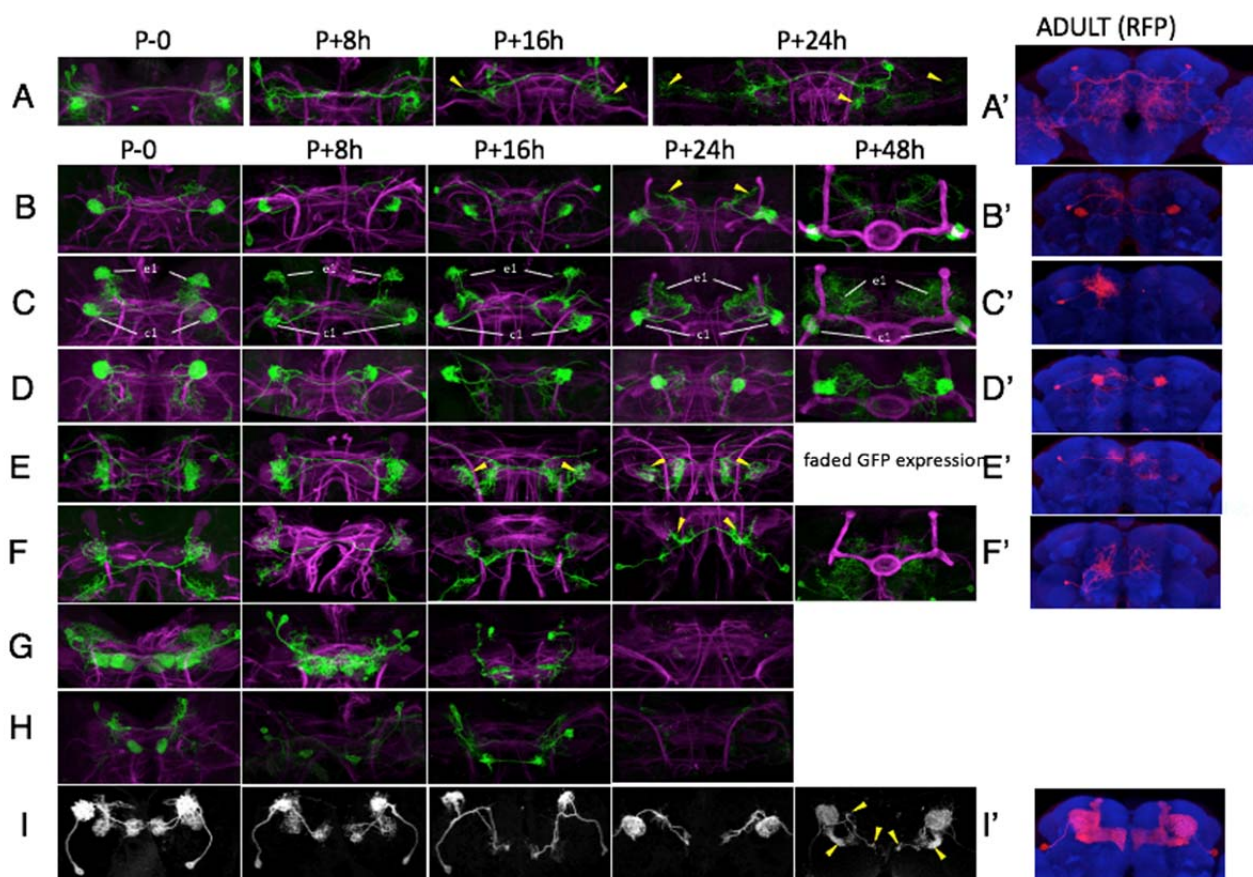
1058 **Figure 3**



1059  
1060  
1061  
1062  
1063  
1064  
1065  
1066  
1067  
1068

**Figure 3. The metamorphic fates of the larval mushroom body output cells (MBONs). (A)** Schematic summarizing the fates of the compartmental MBONs of the larva. Arrows indicate whether cells trans-differentiate to perform non-mushroom body functions in the adult or remodel as MBONs and project from the indicated adult compartments. Lower case letters refer to images in part C. **(B)** Images comparing the larval and adult forms of the larval MBONs based on flip-switch immortalization. The images and names of the larval cells from Saumweber *et al.* 2018; adult names based on Aso *et al.*, 2014 and Li *et al.*, 2020, or this study

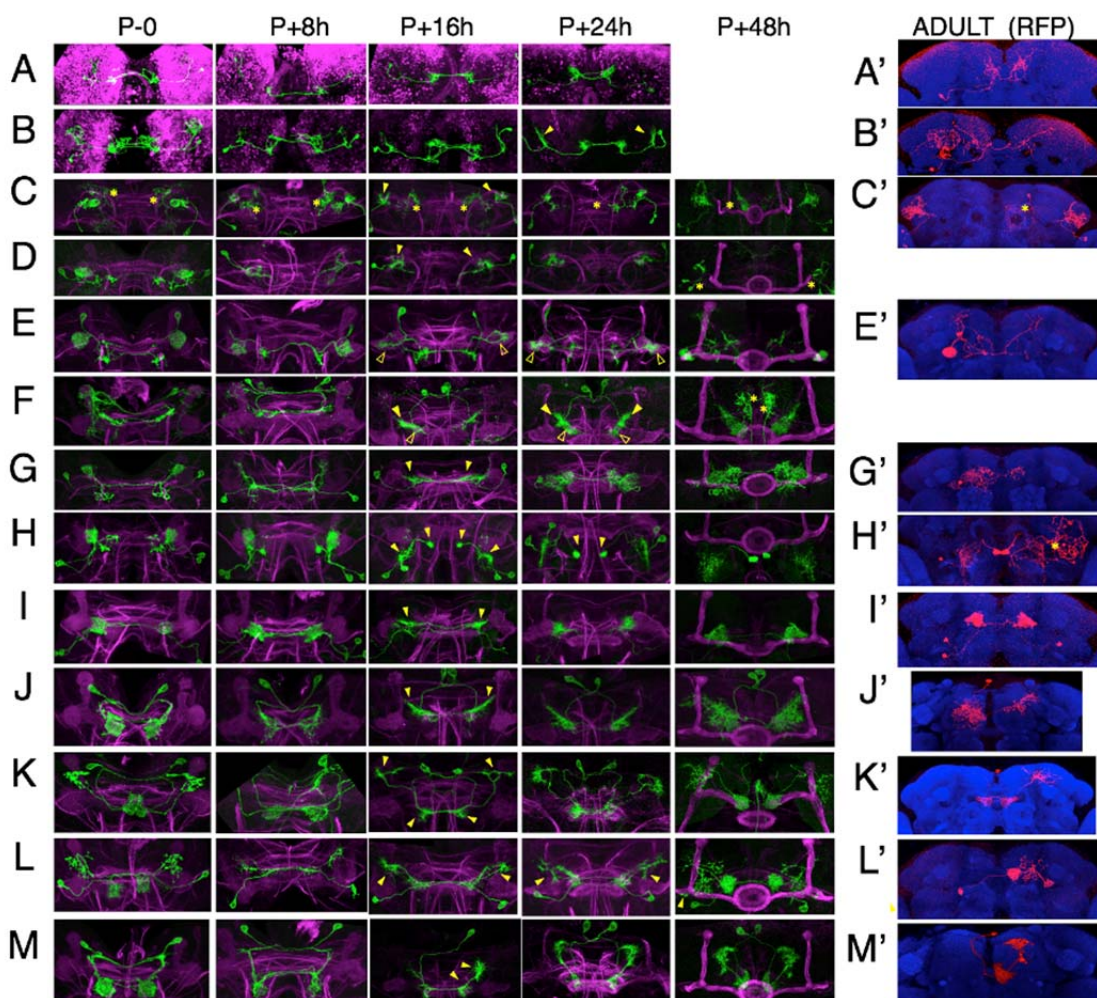
1069 **Figure 4**



1070  
1071  
1072  
1073  
1074  
1075  
1076  
1077  
1078  
1079  
1080  
1081

**Figure 4. Confocal images of the changes in larval MBINs and APL during the first 48 hr of metamorphosis and their adult appearance (').** Confocal images show GFP expression through the early hours of metamorphosis; the adult images show flip-switch induced expression of red fluorescent protein (RFP). Arrow heads: growth cones; \*: contaminating arbor from other cell types. **(A)** MBIN-b1 & -b2 become PAL-OL interneurons. **(B)** DAN-c1 becomes adult PPL1- $\gamma$ 1pedc. **(C)** OAN-e1 becomes PPL1-SMP; this line also expresses in DAN-c1. **(D)** DAN-d1 becomes PPL1- $\gamma$ 2 $\alpha$ '1. **(E)** DAN-g1 becomes PPL1- $\gamma$ 1. **(F)** MBIN-l1 becomes LAL>bi-CRP **(G)** DAN-i1, -j1 and l1 degenerate by 16 to 24 hours after puparium formation (APF). **(H)** DAN-k1 also degenerates. **(I)** APL remodels to become the adult APL. Lines used for developmental timelines: A: JRC-SS21716, B: JRC-SS03066, C: JRC-SS01702, D: JRC-MB328B, E: JRC-SS01716, F: JRC-SS04484, G: JRC-SS-01949, H: JRC-SS01757, I: JRC-SS01671.

1082  
1083



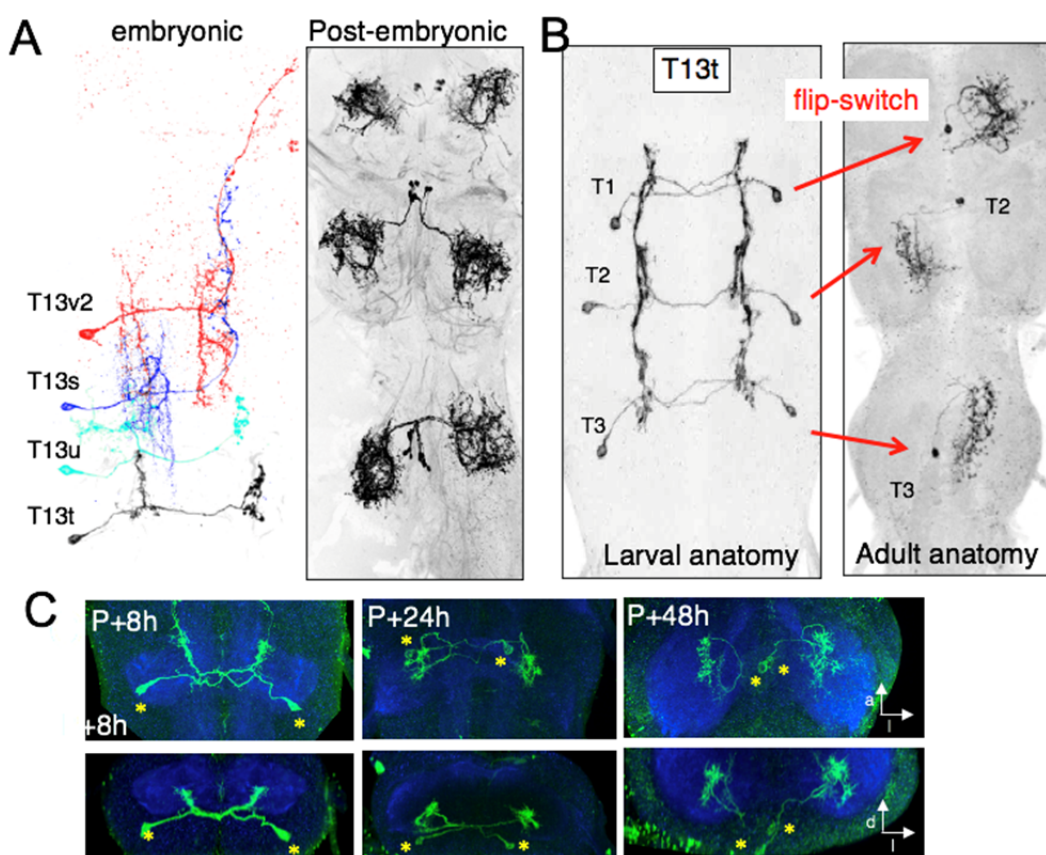
1084 **Figure 5**

1085 **Figure 5. Confocal images of the changes in larval MBONs during the first 48 hours of**  
1086 **metamorphosis and subsequent adult appearance (').** Confocal images show GFP expression  
1087 through the early hours of metamorphosis; the adult images show flip-switch induced expression of red  
1088 fluorescent protein (RFP) showing the terminal anatomy of the cells. Arrow heads: growth cones; \*:  
1089 contaminating arbor from other cell types. **(A)** MBON-a1 becomes MBON 29 ( $\gamma 4, \gamma 5$ ). **(B)** MBON-a1  
1090 becomes adult MBON 22 (MBON calyx). **(C)** MBON-b1 & -b2 become adult lateral horn local neurons.  
1091 **(D)** MBON-c1 becomes MBE-CA. **(E)** MBON-d1 becomes adult MBON 11 ( $\gamma 1$ ped). **(F)** MBON-e2  
1092 becomes MBON 03 ( $\beta 2$ mp). **(G)** MBON f2 becomes MBON 30 ( $\gamma 1\gamma 2\gamma 3$ ). **(H)** MBON-g1 & -g2 become  
1093 the central complex neurons LAL.s-NO<sub>2</sub>i.b. **(I)** MBON-h1 & -h2 become adult MBON 09 ( $\gamma 3\beta'$ 1) and  
1094 MBON 10 ( $\gamma 3$ ). **(J)** MBON-i1 becomes MBON 04 ( $\beta 2$ \_bilat). **(K)** MBON-j1 becomes MBON 02 ( $\beta 2\beta'$ 2a).  
1095 **(L)** MBON-j2 becomes MBON 05 ( $\gamma 4>\gamma 1\gamma 2$ ). **(M)** MBON-k1 becomes MBON 01 ( $\gamma 5\beta'$ 2a). *Drosophila*  
1096 lines used for developmental timelines: A: JRC-SS00867, B: JRC-SS02006, C: JRC-SS01708, D: JRC-  
1097 SS21789, E: JRC-SS01705, F: JRC-SS04559, G: JRC-SS-04320, H: JRC-SS02130, I: JRC-SS01725, J: JRC-  
1098 SS04244, K: JRC-SS01973, L: JRC-SS00860; M: JRC-SS01980.

1099

1100 **Figure 6.**

1101



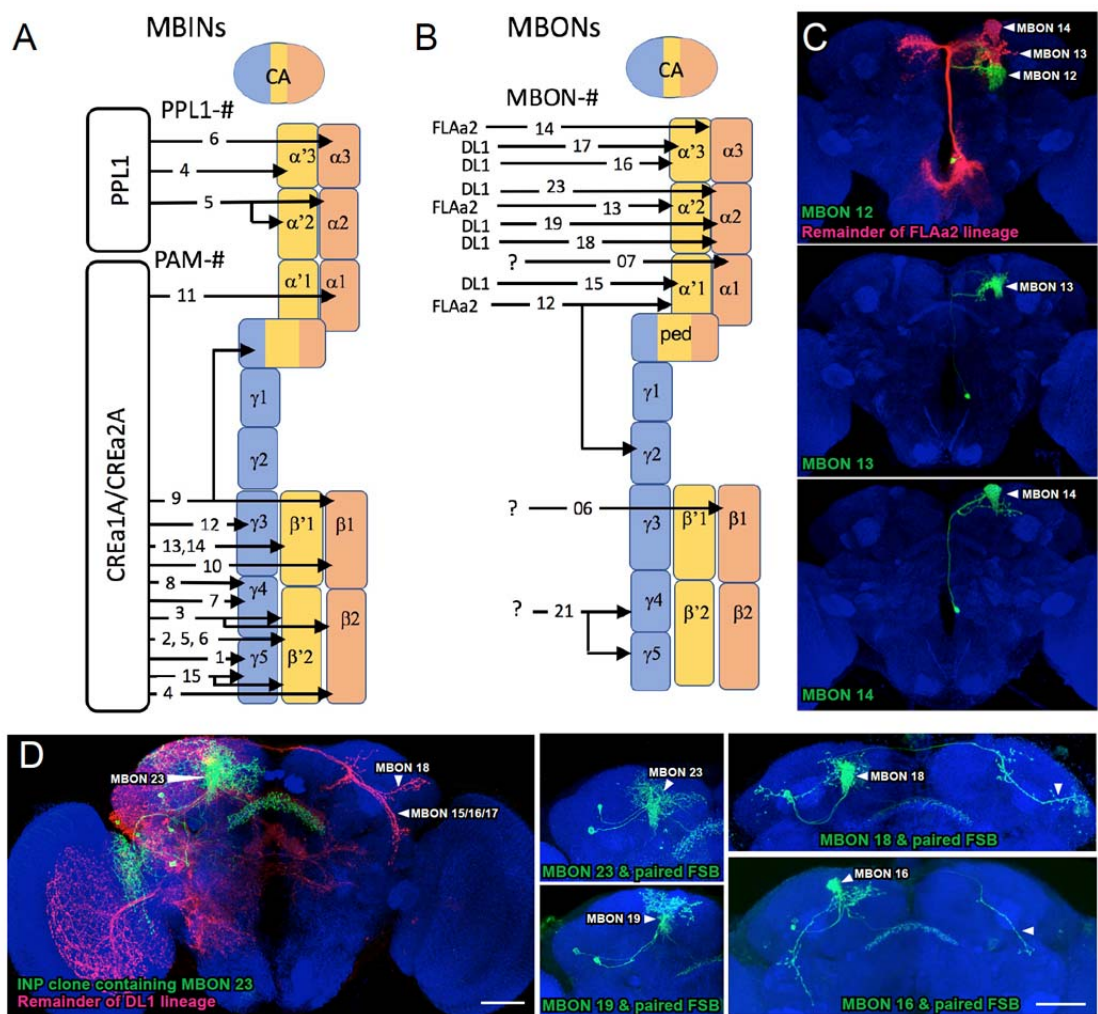
1102  
1103 **Figure 6. Form and fates of lineage 13 (NB4-2) thoracic interneurons.** (A) (Left) staggered images  
1104 of four different lineage 13B larval interneurons in the segment T3; (right) example of the form of the  
1105 postembryonic-born neurons from the same lineage. (B) (Left) image of the larval form of T13t neurons  
1106 revealed by the JRC-SS04274 driver line and (right) examples of the terminal form of these neurons in  
1107 the adult as revealed by the flip-switch method. (C) Dorsal (top) and transverse (bottom) views of the  
1108 early metamorphosis of the T3 pair of T13t cells: the dendritic arbor is gone by 8 hours after pupariation  
1109 (P+8h), contralateral growth cones are evident by P+24h, and the arbor is near its maximal extent by  
1110 P+48h. Through this period, the expanding neuropil pulls the cell bodies (\*) to their adult position near  
1111 the midline.

1112

1113

1114

1115 **Figure 7**



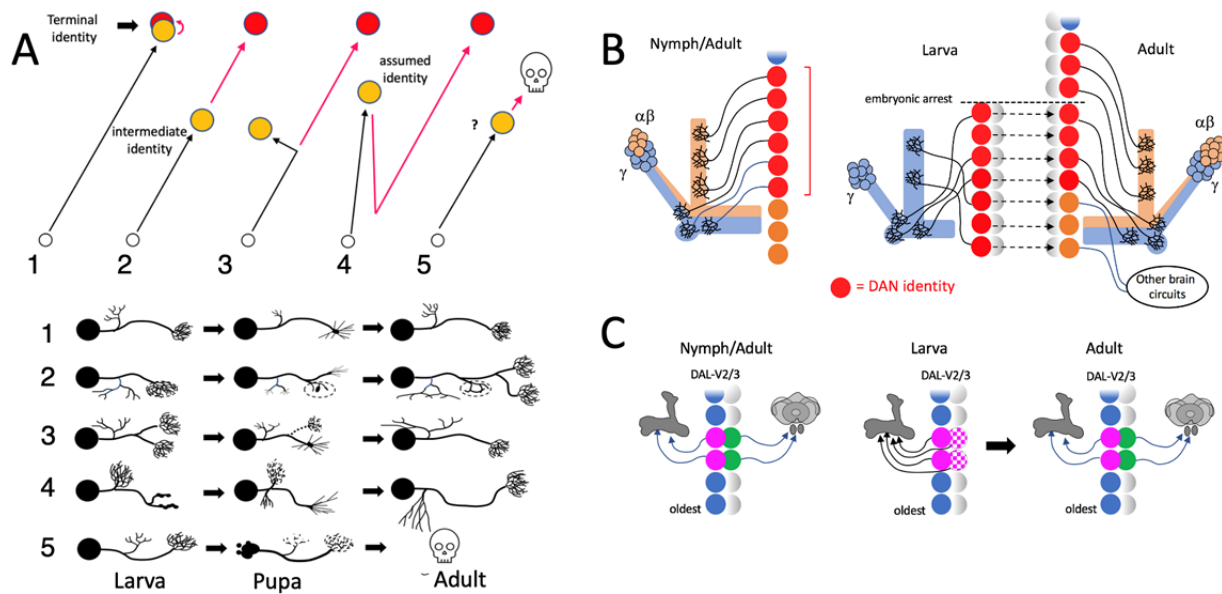
1116  
1117

1118 **Figure 7. The Postembryonic-born MBINs and MBONs of the adult mushroom bodies. (A)**  
1119 Summary of the origins of to the various compartments for the adult mushroom bodies. Numbers give  
1120 the number of neurons in each of the PAM groups (from Aso *et al.*, 2014). **(B)** Summary of the  
1121 postembryonic-born MBONs added to the adult mushroom bodies from the indicated lineages. **(C)**  
1122 Results of twin-spot MARCM approach showing the sequential postembryonic birth of different neurons  
1123 from the FLAa2 lineage which innervate of some the  $\alpha'$  and  $\alpha$  compartments. C, C' and C'' images are  
1124 produced by successively later heat-shocks in the larva; green cells are produced after the heat-shock  
1125 while the red cells (shown only in C) are the remainder of the lineage. **(D)** Twin spot MARCM results  
1126 from type II DL1 lineage. The leftmost panel shows the progeny of an intermediate neural progenitor  
1127 (INP) in green and the remainder of the lineage in green. The remaining panels show GMC clones with  
1128 an MBON neuron and its paired sister fan-shaped body (FSB) neuron.  
1129  
1130

1131  
1132  
1133  
1134  
1135

## Figure 8

Figure 8



1136  
1137

**Figure 8. Cellular strategies for producing larval-adapted neurons.** (A) Schematic comparison of larval (yellow) and adult (red) forms of neurons to illustrate strategies for producing larval cells. The red portion of the path occurs during metamorphosis: (1) neuron acquires its terminal identity by hatching and serves similar roles in larva and adult, (2) larval form is based on an intermediate phase in the development of the neuron's terminal identity. (3) larval and adult cells are similar but larval cell develops significant features that are lost in the adult, (4) the neuron undergoes trans-differentiation in which the larval form has an assumed identity that differs from its adult identity, (5) recruitment of neurons for transient survival in the larva from the populations of neurons that normally die during embryogenesis. (B,C) Potential mechanisms for allowing a trans-differentiating neuron to assume a temporary identity. (B) Generating trans-differentiated PPL1 DAN neurons in the DL2 lineage involves modifying the temporal program that establishes neuron identities within its lineage. In direct developing insects, the PPL1-DANs arise during embryogenesis, as a temporal block of neurons consisting of one daughter cell from each of a sequential series of neuronal precursor cells (red neurons). In *Drosophila*, only some of these neurons are produced before the embryonic neurogenic arrest, but more neurons with the appropriate phenotype are made by temporarily expressing the appropriate determinants in other early-born cells in the lineage. At metamorphosis, these determinants are lost and replaced by ones (orange) characteristic for their terminal identity. (C) Hypothetical scheme in which identity differences between sibs are used to produce temporary larval MBONs in the DAL-V2/3 lineage. In direct developing insects, two sequential neuronal precursors are proposed to divide to produce one daughter directed to the mushroom bodies and the other to the central complex. In larvae of *Drosophila*, the second daughter cell temporarily assumes some of the features of its sibling and re-targets to the larval mushroom body. It assumes its proper central complex role at metamorphosis.

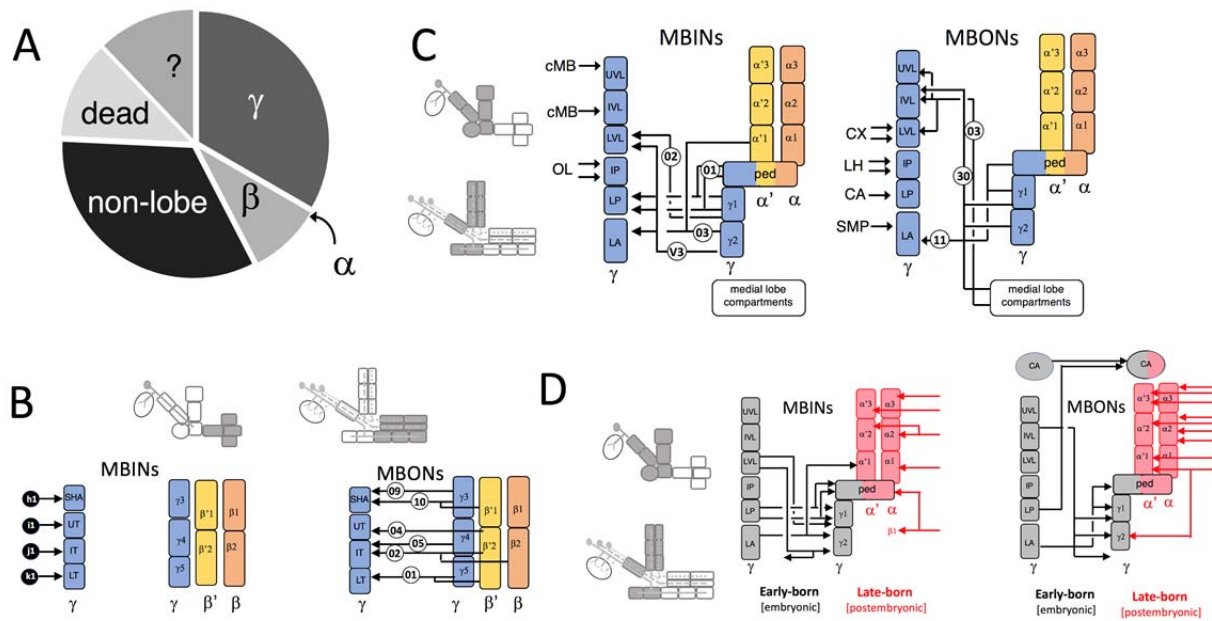
1161

1162 Figure 9

1163

1164

1165



1166

1167 **Figure 9: Comparison of embryonic versus postembryonic origins of the MBINs or**

1168 **MBONs that contribute to the mushroom body compartments of the adult. (A)** A

1169 chart showing the percentage of larval mushroom body MBINs and MBONs that have

1170 different terminal adult fates. A few fates are unknown (?), but the remainder include

1171 death (12%), innervation of adult  $\gamma$  (33%),  $\alpha$  (0%), or  $\beta$  lobe (9%) compartments, or non-

1172 mushroom body circuits (33%). **(B, C)** A schematic summary of the terminal fates of the

1173 neurons innervating various regions of the larval mushroom body. **(B)** the MBINs for the

1174 larval medial lobe compartments are recruited from the population of “doomed” neurons

1175 (black circles), while the MBONs serve similar roles in both the larval and adult structures.

1176 **(C)** the remaining larval compartments are supplied by neurons that assume a temporary

1177 function in the larva and then have a terminal function elsewhere in the brain, or are the

1178 larval forms of adult MBINs or MBONs (adult cell number in circles are as in Fig 2 and 3).

1179 CA: calyx; CX: central complex; cMB: circum-mushroom body neuropil; OL: optic lobe;

1180 SMP: superior medial protocerebrum. **(D)** Developmental origins of the classes of Kenyon

1181 cells that make up the core of the adult mushroom body and the MBINs and MBONs that

1182 innervate this core. The comparison is presented for the compartments of the vertical

1183 lobe, base and peduncle and is based on Figs 2, 3, and 7AB. Embryonic-born classes of

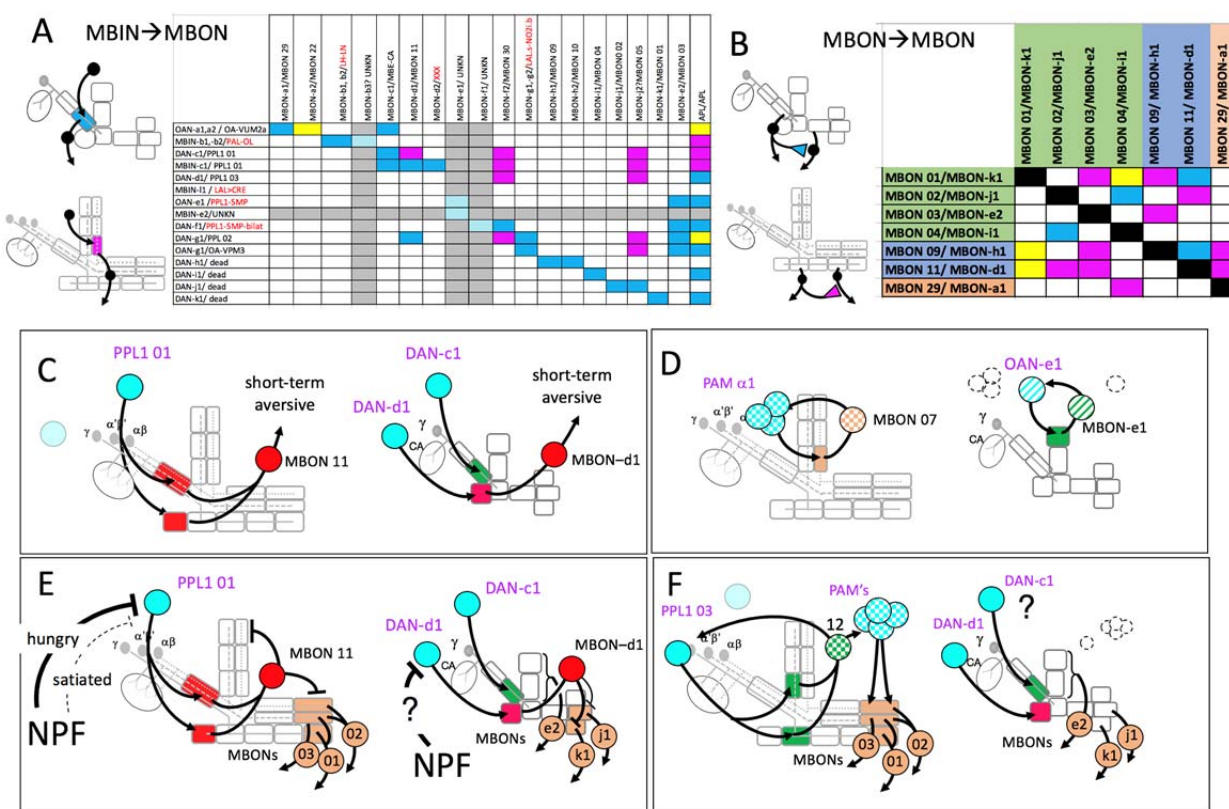
1184 Kenyon cells and their input and output cells are in black while postembryonic-born

1185 Kenyon cells and their input and output cells are in red.

1186

1187  
1188  
1189  
1190  
1191  
1192

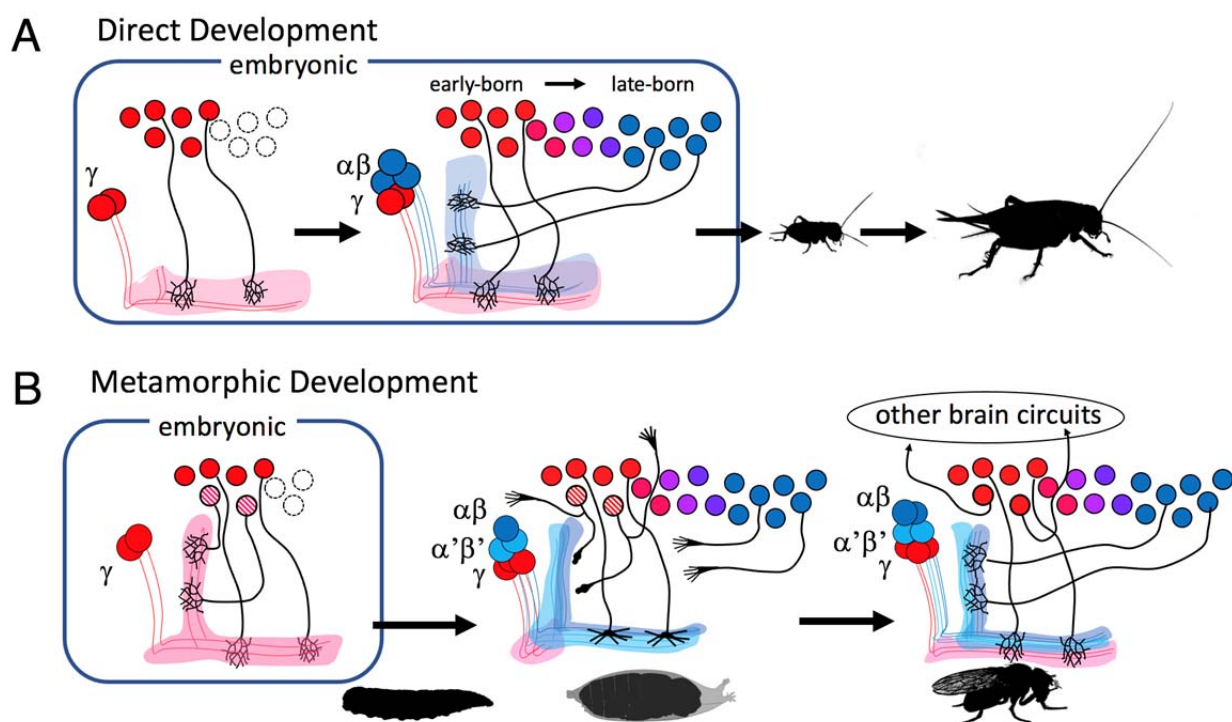
## Figure 10



1193  
1194 **Figure 10 Fate of circuit connections in the mushroom bodies through metamorphosis. (A)**  
1195 Matrix showing the overlap of MBIN axon terminal with MBON dendritic trees in the same  
1196 compartment. Blue: larval pairings; red: adult pairings; yellow: found in both. Cells and columns that  
1197 are grayed out are ones for which the adult identity is unknown. Larval/adult names are provided for  
1198 each cell, with the red names being the terminal identity of neurons that leave the larval mushroom  
1199 bodies. **(B)** Matrix showing the larval (blue) and adult (red) connectivity for a set of MBONs that  
1200 maintain this function through metamorphosis. **(C-F)** comparison of the larval and adult states of circuit  
1201 components for specific examples of adult circuits that illustrate various degrees of learning complexity:  
1202 **(C)** Simple short-term aversive conditioning. **(D)** Consolidation of appetitive conditioning. **(E)** Shift the  
1203 valence of a learned response in response to change in internal state (hunger). **(F)** Re-consolidation and  
1204 extinction of memories based on subsequent experience. Extrinsic neurons with mushroom body  
1205 function only in the larva are cross-hatched and those with adult-specific mushroom body function are  
1206 stippled in the adult and shown as dashed outlines in the larva. Cell body and compartment colors: cyan,  
1207 aminergic; red: GABAergic; green: cholinergic; tan: glutaminergic. See text for details.  
1208  
1209

1210 **Figure 11**

1211



1212  
1213

1214 **Figure 11. The proposed scheme showing the relationship of the development of a single**  
1215 **mushroom body in a direct developing insect to the production of two sequential versions of the**  
1216 **mushroom body in a metamorphic insect like *Drosophila*. (A) In the direct developing insects  $\gamma$**   
1217 **Kenyon cells are made before the  $\alpha\beta$  type Kenyon cells. The  $\gamma$  class generates a medial lobe while the  $\alpha\beta$**   
1218 **classes provide a vertical lobe(s) as well as more medial lobe axons. The timing of birth of the input and**  
1219 **output cells to the Kenyon cell classes is assumed to parallel the relative time of birth of their targets**  
1220 **with those innervating  $\gamma$  neurons being born before those innervating the  $\alpha\beta$  neurons. (B) In the**  
1221 **derived, metamorphic system, typified by *Drosophila*, the early hatching of the larva results in only  $\gamma$**   
1222 **neurons being present, and these possess a novel, vertical axon to make up for the absence of the  $\alpha\beta$**   
1223 **neurons. The input and output cells to the  $\gamma$  neurons are also present at hatching and some of these**  
1224 **assume their expected roles along the larval medial lobe. The larval vertical lobe, though, is analogous,**  
1225 **but not homologous, to the adult structure. Its core is composed of  $\gamma$  cell axons, rather than  $\alpha$  branch**  
1226 **axons, and none of the later-born neurons that innervate  $\alpha$  axons are present at hatching. The role of the**  
1227 **latter neurons is taken over by early-born neurons that trans-differentiate to assume mushroom body**  
1228 **functions in the larva but then revert to their ancestral functions in other brain circuits at**  
1229 **metamorphosis. By this latter time the late-born classes of Kenyon cells and their input and output cells**  
1230 **have been born and an adult mushroom body is formed using the same cell classes as used in their**  
1231 **direct developing relatives.**

1232  
1233  
1234

1235 **Table 1: Metamorphic fates of larval mushroom body extrinsic neurons.**

1236

1237

Larval name	compartment	lineage [*]	Adult identity	ref for adult identity
<b>MBINs</b>				
OAN-a1,a2	CX	undetermined	OA-VUM2a	Busch <i>et al.</i> , 2009
MBIN-b1,b2	IP	DPLd	PAL-OL	Mao & Davis, 2009; this study
DAN-c1	LP	CPd2/3	PPL1 01 ( $\gamma 1$ pedc)	Aso <i>et al.</i> , 2014; Li <i>et al.</i> , 2020
MBIN-c1	LP	CPd2/3	PPL1 01 ( $\gamma 1$ pedc)	Aso <i>et al.</i> , 2014; Li <i>et al.</i> , 2020
DAN-d1	LA	CPd2/3	PPL1 03 ( $\gamma 2\alpha'1$ )	Aso <i>et al.</i> , 2014; Li <i>et al.</i> , 2020
MBIN-l1	LA	BLV a3/4	LAL>bi-CRP	This study
OAN-e1	UVL	CPd2/3	PPL1-SMP	Mao & Davis, 2009; this study
MBIN-e2	UVL	CPd2/3	unknown	
DAN-f1	IVL	CPd2/3	PPL1-bi-SMP	Mao & Davis, 2009; this study
DAN-g1	LVL	CPd2/3	PPL1 02 ( $\gamma 1$ )	Aso <i>et al.</i> , 2014; Li <i>et al.</i> , 2020
OAN-g1	LVL	undetermined	OA-VPM3	Busch <i>et al.</i> , 2009
DAN-h1	SHA	DAL CM-1/2	dead	This study
DAN-i1	UT	DAL CM-1/2	dead	This study
DAN-j1	IT	DAL CM-1/2	dead	This study
DAN-k1	LT	DAL CM-1/2	dead	This study
<b>MBONs:</b>				
MBON-a1	CX	CPv2/3	MBON 29 ( $\gamma 4\gamma 5$ )	This study
MBON-a2	CX	CPv2/3	MBON 22 (calyx)	Aso <i>et al.</i> , 2014; Li <i>et al.</i> , 2020
MBON-b1,b2	IP	BLVa3/4	LH-LN	Dolan <i>et al.</i> , 2019
MBON-b3	IP	CPv2/3	unknown	
MBON-c1	LP	BLDc	MBEN-CA	This study
MBON-d1	LA	DAL CM-1/2	MBON 11 ( $\gamma 1$ pedc> $\alpha/\beta$ )	Aso <i>et al.</i> , 2014; Li <i>et al.</i> , 2020
MBON-d2	LA	BAmd2	SMP>IB	This study
MBON-e1	UVL	CPd2/3	unknown	
MBON-f2	IVL	DAL cl2	MBON 30 ( $\gamma 1,\gamma 2,\gamma 3$ )	Li <i>et al.</i> , 2020
MBON-f1	IVL	CPd	unknown	
MBON-g1,g2	LVL	DAL-V2/3	LAL-s-NO <sub>2</sub> i.b	Wolff & Rubin, 2018
MBON-h1	SHA	DAL-V2/3	MBON 09 ( $\gamma 3\beta'1$ )	Aso <i>et al.</i> , 2014; Li <i>et al.</i> , 2020
MBON-h2	SHA	DAL-V2/3	MBON 10 ( $\gamma 3$ )	Aso <i>et al.</i> , 2014; Li <i>et al.</i> , 2020
MBON-i1	UT	DAM-d1	MBON 04 ( $\beta'2$ -bilat)	Aso <i>et al.</i> , 2014; Li <i>et al.</i> , 2020
MBON-j1	IT	DAM-d1	MBON 02 ( $\beta 2\beta'2a$ )	Aso <i>et al.</i> , 2014; Li <i>et al.</i> , 2020
MBON-j2	IT	DAL CM-1/2	MBON 05 ( $\gamma 4>\gamma 1,\gamma 2$ )	Aso <i>et al.</i> , 2014; Li <i>et al.</i> , 2020
MBON-k1	LT	DAM-d1	MBON 01 ( $\gamma 5\beta'2a$ )	Aso <i>et al.</i> , 2014; Li <i>et al.</i> , 2020
MBON-e2	UVL, IVL, LVL	DAM-d1	MBON 03 ( $\beta'2mp$ )	Aso <i>et al.</i> , 2014; Li <i>et al.</i> , 2020
APL	UT,LT,LA, VL>CX	BLV a3/4	APL	Aso <i>et al.</i> , 2014; Li <i>et al.</i> , 2020

1238

1239 \*Lineage designations from Saumweber *et al.*, 2018. CX: calyx; IP: intermediate peduncle; LP: lower  
 1240 peduncle; UVL: upper vertical lobe; IB: inferior bridge; IVL: intermediate vertical lobe; LVL: lower  
 1241 vertical lobe; LA: lateral appendix; OT: optic tubercle; SHA: shaft; SMP: superior medial protocerebrum;  
 1242 UT: upper toe; IT: intermediate toe; LT: lower toe.

1243

1244

1245

1246 **Table 2: Developmental origins of adult MBINs and MBONs that do not come from remodeled**  
 1247 **larval, extrinsic mushroom body neurons.**  
 1248

Cell Name	Alternate name	#	origin	lineage	reference
<b>MBINs</b>					
PPL1-06	PPL1- $\alpha$ 3	1	postembryonic	DL2	Ren <i>et al.</i> , 2016
PPL1-05	PPL1- $\alpha$ '2 $\alpha$ 2	1	postembryonic	DL2	Ren <i>et al.</i> , 2016
PPL1-04	PPL1- $\alpha$ '3	1	postembryonic	DL2	Ren <i>et al.</i> , 2016
PAM01	PAM- $\gamma$ 5	19	postembryonic	CREa1A, CREa2A [P]	Lee <i>et al.</i> , 2020
PAM04	PAM- $\beta$ 2	16	postembryonic	CREa1A, CREa2A [P]	Lee <i>et al.</i> , 2020
PAM05	PAM- $\beta$ '2p	10	postembryonic	CREa1A, CREa2A [P]	Lee <i>et al.</i> , 2020
PAM02	PAM- $\beta$ '2a	8	postembryonic	CREa1A, CREa2A [P]	Lee <i>et al.</i> , 2020
PAM03	PAM- $\beta$ 2 $\beta$ '2a	4	postembryonic	CREa1A, CREa2A [P]	Lee <i>et al.</i> , 2020
PAM06	PAM- $\beta$ '2m	15	postembryonic	CREa1A, CREa2A [P]	Lee <i>et al.</i> , 2020
PAM07	PAM- $\gamma$ 4 $\gamma$ 1 $\gamma$ 2	5	postembryonic	CREa1A, CREa2A [P]	Lee <i>et al.</i> , 2020
PAM08	PAM- $\gamma$ 4	26	postembryonic	CREa1A, CREa2A [P]	Lee <i>et al.</i> , 2020
PAM10	PAM- $\beta$ 1	6	postembryonic	CREa1A, CREa2A [P]	Lee <i>et al.</i> , 2020
PAM11	PAM- $\alpha$ 1	7	postembryonic	CREa1A, CREa2A [P]	Lee <i>et al.</i> , 2020
PAM12	PAM- $\gamma$ 3	11	postembryonic	CREa1A, CREa2A [P]	Lee <i>et al.</i> , 2020
PAM13	PAM- $\beta$ '1ap	7	postembryonic	CREa1A, CREa2A [P]	Lee <i>et al.</i> , 2020
PAM14	PAM- $\beta$ '1	8	postembryonic	CREa1A, CREa2A [P]	Lee <i>et al.</i> , 2020
PAM09	PAM- $\beta$ 1ped	6	postembryonic	CREa1A, CREa2A [P]	Lee <i>et al.</i> , 2020
PAM15	PAM- $\gamma$ 5 $\beta$ '2a	3	postembryonic	CREa1A, CREa2A [P]	Lee <i>et al.</i> , 2020
	PAM $\gamma$ 4/5	?	postembryonic	CREa1A, CREa2A [P]	Lee <i>et al.</i> , 2020
<b>MBONs</b>					
MBON 07	MBON- $\alpha$ 1 [2]	2	ND		
MBON 17	MBON- $\alpha$ '3m [2]	2	postembryonic	DL1	this study
MBON 06	MBON- $\beta$ 1> $\alpha$ [1]	1	ND		
MBON 15	MBON- $\alpha$ '1 (2)	2	postembryonic	DL1	this study
MBON 12	MBON- $\gamma$ 2 $\alpha$ '1 (2)	2	postembryonic	FLAa2	this study
MBON 16	MBON- $\alpha$ '3ap (1)	1	postembryonic	DL1	this study
MBON 18	MBON- $\alpha$ 2sc (1)	1	postembryonic	DL1	this study
MBON 13	MBON- $\alpha$ '2 (1)	2	postembryonic	FLAa2	this study
MBON 19	MBON $\alpha$ 2p3p (2)	2	postembryonic	DL1	this study
MBON 14	MBON- $\alpha$ 3 (2)	2	postembryonic	FLAa2	this study
MBON 21	MBON- $\gamma$ 4, $\gamma$ 5	1	ND		
MBON 23	MBON- $\alpha$ 2sp	1	postembryonic	DL1	this study
DPM	MB-DPM	1	postembryonic	undetermined	Mayseless <i>et al.</i> , 2018

1249  
 1250  
 1251 Adult names according to Aso *et al.*, 2014 and Li *et al.*, 2020, except PAM  $\gamma$ 4/5 which is based on Lee *et*  
 1252 *al.*, 2020.  
 1253  
 1254

1255  
1256

**Table 3 : Comparison of transmitter expression in larval and adult forms of MBONs and MBINs**

Larval name	larval transmitt	Adult name	adult transmitter	larval ref	adult ref
<b>MBINs</b>					
OAN-a1,a2	octopamine	OA-VUM2a	octopamine	Eichler <i>et al.</i> , 2017	Busch <i>et al.</i> , 2009
MBIN-b1,b2	TH-positive	PAL-OL	TH-positive	Eichler <i>et al.</i> , 2017	Mao & Davis, 2009; this study
DAN-c1	dopamine	PPL1 01 [PPL1- $\gamma$ 1pedc]	dopamine	Eichler <i>et al.</i> , 2017	Aso <i>et al.</i> , 2014 [Li <i>et al.</i> , 2020]
MBIN-c1	putative dopamine	PPL1 01 [PPL1- $\gamma$ 1pedc]	dopamine	Eichler <i>et al.</i> , 2017	Aso <i>et al.</i> , 2014 [Li <i>et al.</i> , 2020]
DAN-d1	dopamine	PPL1 03 {PPL1- $\gamma$ 2 $\alpha$ '1} [PPL103]	dopamine	Eichler <i>et al.</i> , 2017	Aso <i>et al.</i> , 2014 [Li <i>et al.</i> , 2020]
MBIN-11	TH-positive	TD_LAL>cre	undetermined	Eichler <i>et al.</i> , 2017	
OAN-e1	octopamine	PPL1-SMP	TH-positive	Eichler <i>et al.</i> , 2017	Mao & Davis, 2009
DAN-f1	dopamine	PPL1-bilat	TH-positive	Eichler <i>et al.</i> , 2017	Mao & Davis, 2009
DAN-g1	dopamine	PPL1 02 [PPL1- $\gamma$ 1]	dopamine	Eichler <i>et al.</i> , 2017	Aso <i>et al.</i> , 2014 [Li <i>et al.</i> , 2020]
OAN-g1	octopamine	OA-VPM3	octopamine	Eichler <i>et al.</i> , 2017	Busch <i>et al.</i> , 2009
<b>MBONs:</b>					
MBON-a1	acetylcholine	MBON 29 (MBON $\gamma$ 4 $\gamma$ 5)	undetermined	Eichler <i>et al.</i> , 2017	
MBON-a2	acetylcholine	MBON 22 (MBON calyx)	putative acetylcholine	Eichler <i>et al.</i> , 2017	Li <i>et al.</i> , 2020
MBON-b1,b2	GABA	LH-LN	putative GABA	acetylcholine	Dolan <i>et al.</i> , 2019
MBON-c1	acetylcholine	MBE-CA	unknown	Eichler <i>et al.</i> , 2017	
MBON-d1	GABA	MBON- $\gamma$ 1pedc> $\alpha$ / $\beta$ [MBON 11]	GABA	acetylcholine	Aso <i>et al.</i> , 2014 [Li <i>et al.</i> , 2020]
MBON-d2	undetermined	OT-SMP>IB	unknown		This study
MBON-e1	acetylcholine	unknown		Eichler <i>et al.</i> , 2017	
MBON-e2	glutamate	MBON 03 (MBON- $\beta$ '2mp)	glutamate	Eichler <i>et al.</i> , 2017	Aso <i>et al.</i> , 2014 [Li <i>et al.</i> , 2020]
MBON-f2	undetermined	MBON 30 (MBON- $\gamma$ 1, $\gamma$ 2, $\gamma$ 3)	putative glutamate		Li <i>et al.</i> , 2020
MBON-g1,g2	GABA	LAL-s-NO <sub>2</sub> i.b	undetermined	Eichler <i>et al.</i> , 2017	
MBON-h1	GABA	MBON 09 [MBON- $\gamma$ 3 $\beta$ '1]	GABA	Eichler <i>et al.</i> , 2017	Aso <i>et al.</i> , 2014 [Li <i>et al.</i> , 2020]
MBON-h2	GABA	MBON 10 [MBON- $\gamma$ 3]	GABA		
MBON-i1	glutamate	MBON 04 [MBON- $\beta$ '2-bilat]	glutamate	Eichler <i>et al.</i> , 2017	Aso <i>et al.</i> , 2014 [Li <i>et al.</i> , 2020]
MBON-j1	glutamate	MBON 02 [MBON- $\beta$ 2 $\beta$ '2a]	glutamate	Eichler <i>et al.</i> , 2017	Aso <i>et al.</i> , 2014 [Li <i>et al.</i> , 2020]
MBON-j2	glutamate	MBON 05 [MBON- $\gamma$ 4> $\gamma$ 1, $\gamma$ 2]	glutamate	Saumweber <i>et al.</i> , 2018	Aso <i>et al.</i> , 2014 [Li <i>et al.</i> , 2020]
MBON-k1	glutamate	MBON 01 [MBON- $\gamma$ 5 $\beta$ '2a]	glutamate	Eichler <i>et al.</i> , 2017	Aso <i>et al.</i> , 2014 [Li <i>et al.</i> , 2020]
APL	GABA	MB-APL	GABA	working on these	Aso <i>et al.</i> , 2014 [Li <i>et al.</i> , 2020]

1257  
1258  
1259

1260 **Table 4. Lines used to determine fates of larval neurons**

Cell name	split line	split line	split line
MBIN-b1,b2	<b>SS21716 (FS, TL)</b>		
DAN-c1	<b>SS03066 (FS, TL)</b>	<b>MB586B (FS)</b>	SS01702 (FS)
DAN-d1	<b>MB328B (FS, TL)</b>		
MBIN-i1	<b>SS04484 (FS, TL)</b>	SS01624 (FS)	
OAN-e1	<b>SS36923 (FS)</b>	SS01958 (FS)	
DAN-f1 (+ DAN-c1)	<b>MB065b (FS, TL)</b>	MB145 (TL)	
DAN-g1	<b>SS01716 (FS, TL)</b>	SS01755 (FS)	
OAN-g1 (sVPMmx)	<b>SS25844 (FS)</b>	<b>SS04268 (FS)</b>	
DAN-h1	<b>SS01949 (NC,TL)</b>	SS01696 (NC)	MB440B (NC)
DAN-i1	<b>SS01949 (NC,TL)</b>	MB196C (NC)	
DAN-j1	<b>SS01949 (NC,TL)</b>	MB316B (NC)	MB340C (NC)
DAN-k1	<b>SS01757 (NC,TL)</b>	MB198B (NC)	SS00616 (NC)
MBON-a1	<b>SS00867 (FS,TL)</b>	<b>SS01417 (FS)</b>	
MBON-a2	<b>SS02006 (FS)</b>		
MBON-b1,b2	<b>SS01708 (FS, TL)</b>	<b>SS04112 (FS)</b>	SS01959 (FS)
MBON-c1	SS21789 (FS, TL)		
MBON-d1	<b>SS01705 (FS,TL)</b>		
MBON-d2	<b>SS04231 (FS)</b>		
MBON-e2	SS04559 (FS, TL)		
MBON-f2	<b>SS04328 (FS, TL)</b>	SS36248 (FS)	
MBON-g1,g2	<b>SS02130 (FS, TL)</b>	SS02121 (FS)	
MBON-h1,h2	<b>SS01725 (FS, TL)</b>		
MBON-i1	SS01771		
MBON-j1	<b>SS01973 (FS,TL)</b>	SS01972 (FS)	
MBON-j2	<b>SS00860 (FS,TL)</b>		
MBON-k1	<b>SS01962 (FS)</b>	<b>SS01980 (TL)</b>	
APL	<b>SS01671 (FS, TL)</b>		

1261  
1262  
1263  
1264  
1265

FS: flip-switch immortalization; NC: no adult counterpart; TL: developmental timeline. **Bold** lines were the best lines for each cell.

1266  
1267

**Table 5. Split GAL4 lines used in study**

split line	target cell	AD	DBD
<b>MB065b</b>	DAN-f1 (+ DAN-c1)	TH-p65ADZp in attP40	R72B05-ZpGdbd in attP2
<b>MB145</b>	DAN-f1 (+ DAN-c1)	R15B01-p65ADZp in attP40	R72B05-ZpGdbd in attP2
MB 196C	DAN-i1	R58E02-p65ADZp in attP40	R36B06-ZpGdbd in attP2
MB198B	DAN-k1	R58E02-p65ADZp in attP40	R71D01-ZpGdbd in attP2
MB316B	DAN-j1	R58E02-p65ADZp in attP40	R93G08-ZpGdbd in attP2
<b>MB328B</b>	DAN-d1	R82C10-p65ADZp in attP40	R32F01-ZpGdbd in attP2
MB340C	DAN-j1	R93D10-p65ADZp in attP40	R12G04-ZpGdbd in attP2
MB440B	DAN-h1	R30G08-p65ADZp in attP40	R17D06-ZpGdbd in attP2
<b>MB586B</b>	DAN-c1	TH-p65ADZp in attP40	R72G06-ZpGdbd in attP2
SS00616	DAN-k1	71D01-p65ADZp in VK00027	17D06-ZpGdbd in attP2
<b>SS00860</b>	MBON-j2	w; R89G07-p65ADZ; MKRS/TM6B	R24E12-ZpGdbd in attP2
<b>SS00867</b>	MBON-a1	w; R93G12-p65ADZ; MKRS/TM6B	R52E12-ZpGdbd in attP2
<b>SS01417</b>	MBON-a1	w; R52E12-p65ADZp	R93G12-ZpGdbd in attP2
SS01624	MBIN-I1	w; R84D07-p65ADZ	R37G09-ZpGdbd in attP2
<b>SS01671</b>	APL	R21D02-p65ADZp	R55D08-ZpGdbd in attP2
SS01696	DAN-h1	76F05-p65ADZp in attP40	95H02-ZpGdbd in attP2
SS01702	DAN-c1	VT054895-p65ADZ in attP40	R53C05-ZpGdbd in attP2
<b>SS01705</b>	MBON-d1	R11E07-p65ADZp in attP40	R52H01-ZpGdbd in attP2
<b>SS01708</b>	MBON-b1,b2	R12G03-p65ADZp in attP40	21D02-ZpGdbd in attP2
<b>SS01716</b>	DAN-g1	R14E06-p65ADZp in attP40	R27G01-ZpGdbd in attP2
<b>SS01725</b>	MBON-h1,h2	R20A02-p65ADZp in attP40; MKRS/TM6B	R28A10-ZpGdbd in attP2
SS01755	DAN-g1	R46F09-p65ADZp	R14E06-ZpGdbd in attP2
<b>SS01757</b>	DAN-k1	w; R48F09-p65ADZp; MKRS/TM6B	R27A11-ZpGdbd in attP2
SS01771	MBON-i1	w; 65A05-p65ADZ; MKRS/TM6B	14C08-ZpGdbd in attP2
<b>SS01949</b>	DAN-h1, -i1, -j1	VT026700-p65ADZp in attP40	VT058464-ZpGDBD in attP2
SS01958	OAN-e1	VT023826-p65ADZp in attP40	R75F01-ZpGdbd in attP2
SS01959	MBON-b1,b2	VT027952-p65ADZp in attP40	R26A02-ZpGdbd in attP2
<b>SS01962</b>	MBON-k1	VT033301-p65ADZp in attP40	R27G01-ZpGdbd in attP2
SS01972	MBON-j1	VT057469-p65ADZp in attP40	12C11-ZpGdbd/TM3 in attP2
<b>SS01973</b>	MBON-j1	VT057469-p65ADZp in attP40	R18D09-ZpGdbd in attP2
<b>SS01980</b>	MBON-k1	VT020613-p65ADZp in attP40	VT033301-ZpGdbd in attP2
<b>SS02006</b>	MBON-a2	w; 93G12-p65ADZ; MKRS/TM6B	71E06-ZpGdbd in attP2
SS02121	MBON-g1,g2	R21D06-p65ADZp in attP40	R23B09-ZpGdbd in attP2
<b>SS02130</b>	MBON-g1,g2	w; R23B09-p65ADZp; MKRS/TM6B	R21D06-ZpGdbd in attP2
<b>SS03066</b>	DAN-c1	VT054895-p65ADZ in attP40	VT057278-ZpGdbd in attP2
<b>SS04112</b>	MBON-b1,b2	VT027952-p65ADZp in attP40	HAV5; CyO/Sco; 21D02-ZpGDBD in attP2
<b>SS04231</b>	MBON-d2	VT032899-p65ADZp in attP40	HAV5; CyO/Sp; 87G02-ZpGDBD in attP2
<b>SS04268</b>	OAN-g1 (sVPMmx)	VT012639-p65ADZp in attP40	VT016127-ZpGdbd in attP2
<b>SS04328</b>	MBON-f2	VT033301-p65ADZp in attP40	VT029593-ZpGdbd in attP2
<b>SS04484</b>	MBIN-I1	R37G09-p65ADZp in attP40	VT007174-ZpGdbd in attP2
<b>SS21716</b>	MBIN-b1,b2	VT048835-p65ADZp in attP40	VT026664-ZpGdbd in attP2
SS21789	MBON-c1	VT050247-p65ADZp in attP40	VT050247-ZpGDBD in attP2
<b>SS25844</b>	OAN-g1 (sVPMmx)	VT040569-p65ADZp in attP40	VT061921-ZpGdbd in attP2
SS36248	MBON-f2	VT016795-p65ADZ in attP40	VT029593-ZpGdbd in attP2
<b>SS36923</b>	OAN-e1	VT054895-p65ADZ in attP40	HAV5; CyO/Sco; 75F01-ZpGDBD in attP2
SS04559	MBON-e2	w; 65A05-p65ADZ; MKRS/TM6B	VT045663-ZpGDBD in attP2

1268  
1269

1270  
1271

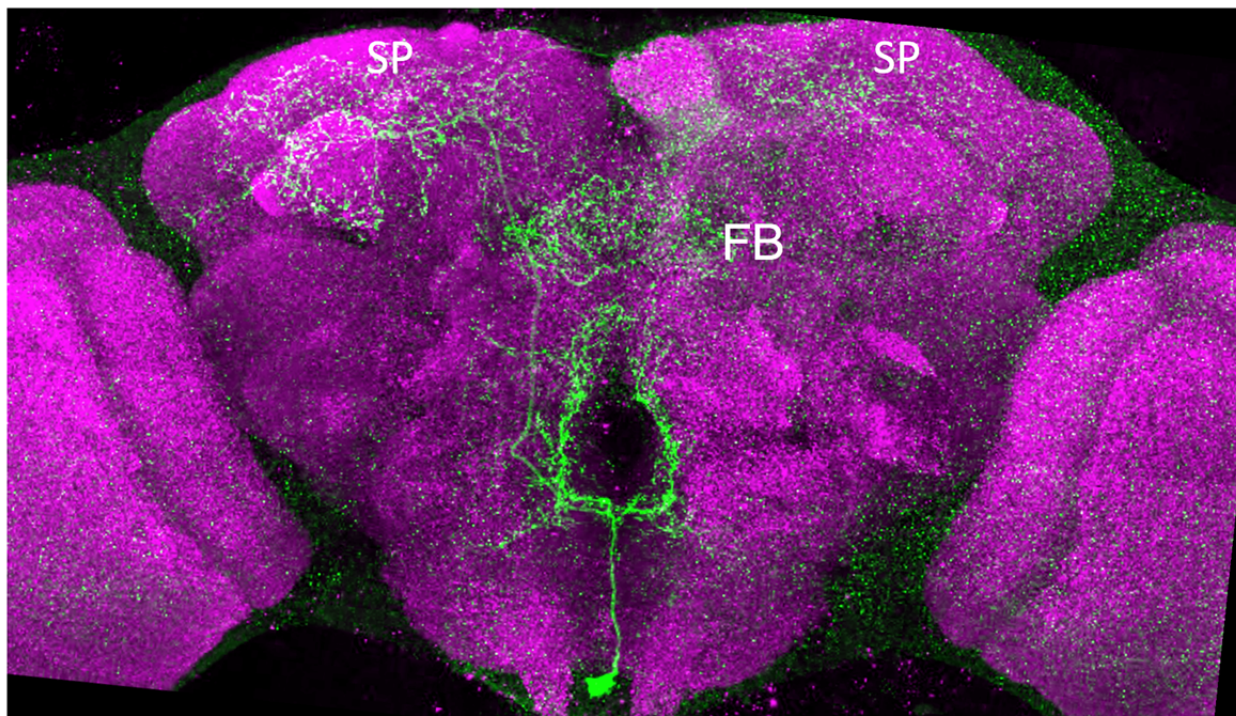
**Table 6: Reagents used in the present study.**

Reagent	Source	Catalog number
Mouse anti-bruchpilot	Developmental Studies Hybridoma Bank	nc82-s
Rat anti-N cadherin	Developmental Studies Hybridoma Bank	DN-Ex #8
Mouse anti-neuroglian	Developmental Studies Hybridoma Bank	BP 104
Mouse anti-Fasciclin II	Developmental Studies Hybridoma Bank	1D4
Rabbit anti-DsRed	ClonTech	#632496
Normal Donkey Serum	Jackson ImmunoResearch	#017-000-121
AF488 Donkey $\alpha$ -rabbit	Jackson ImmunoResearch	#711-545-152
AF488 Donkey $\alpha$ -Mouse	Jackson ImmunoResearch	#711-585-151
AF594 Donkey $\alpha$ -Rabbit	Jackson ImmunoResearch	#711-585-152
AF594 Donkey $\alpha$ -Mouse	Jackson ImmunoResearch	#715-585-151
AF649 Donkey $\alpha$ -Rat	Jackson ImmunoResearch	#712-605-153
Mifepristone (RU-486), $\geq 98\%$ .	Sigma Aldrich	#M8046-100MG
S2 – Schneider's Insect Medium	Sigma Aldrich	#S01416
DPX mountant	Electron Microscopy Sciences	# 13512

1272  
1273

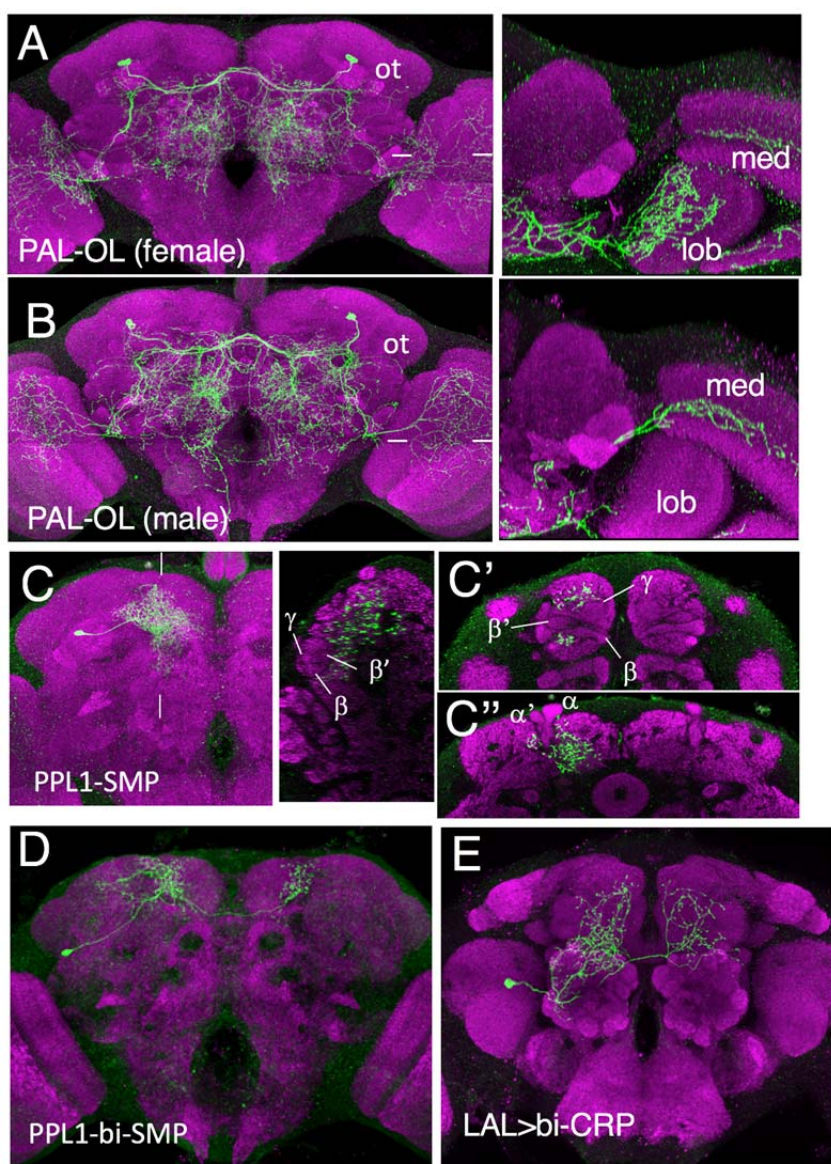
1274  
1275  
1276

## Supplemental Figures



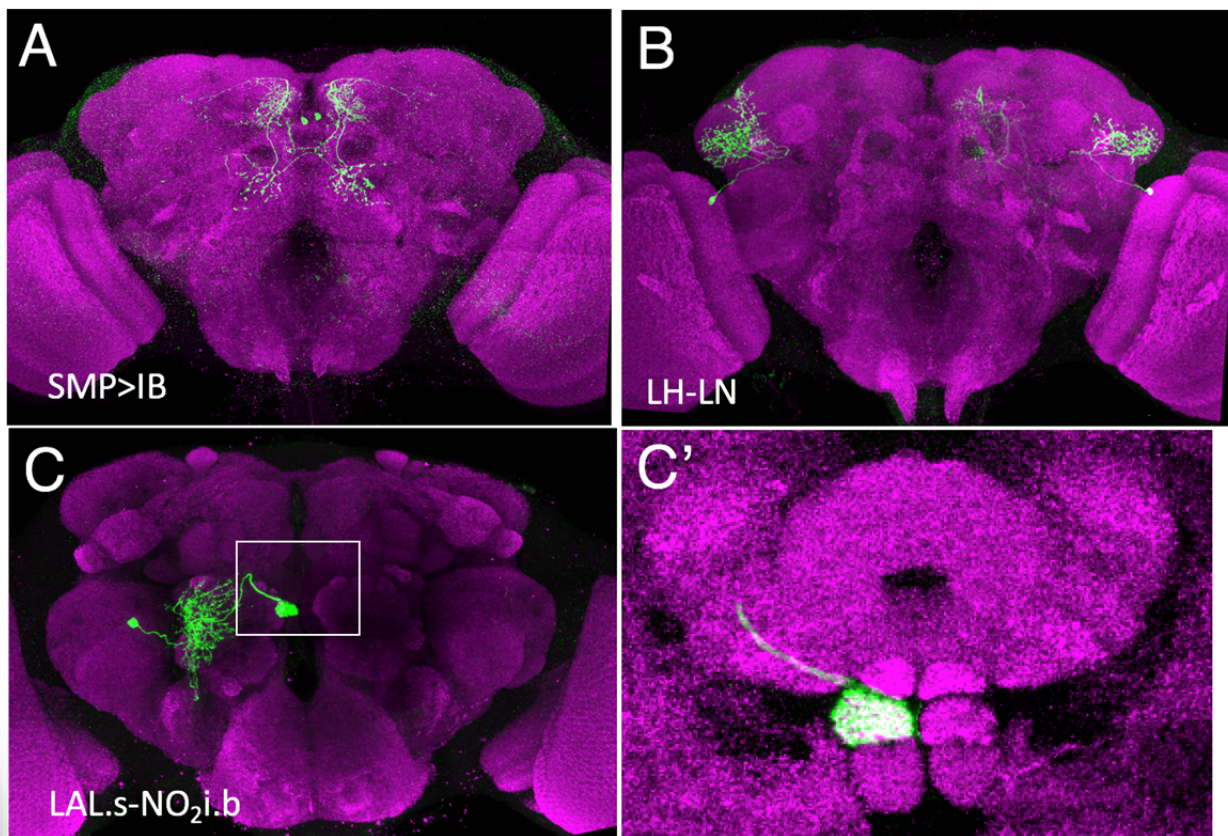
1277  
1278  
1279  
1280  
1281  
1282  
1283  
1284

**Figure 2---figure supplement 1.** Confocal projections showing the terminal, adult structure of the larval neuron OAN-g1. The adult cell is called OA-VPM3. FB: fan shaped body; SP: superior protocerebrum. Green: pseudo color representation of RFP; Magenta: nc82.

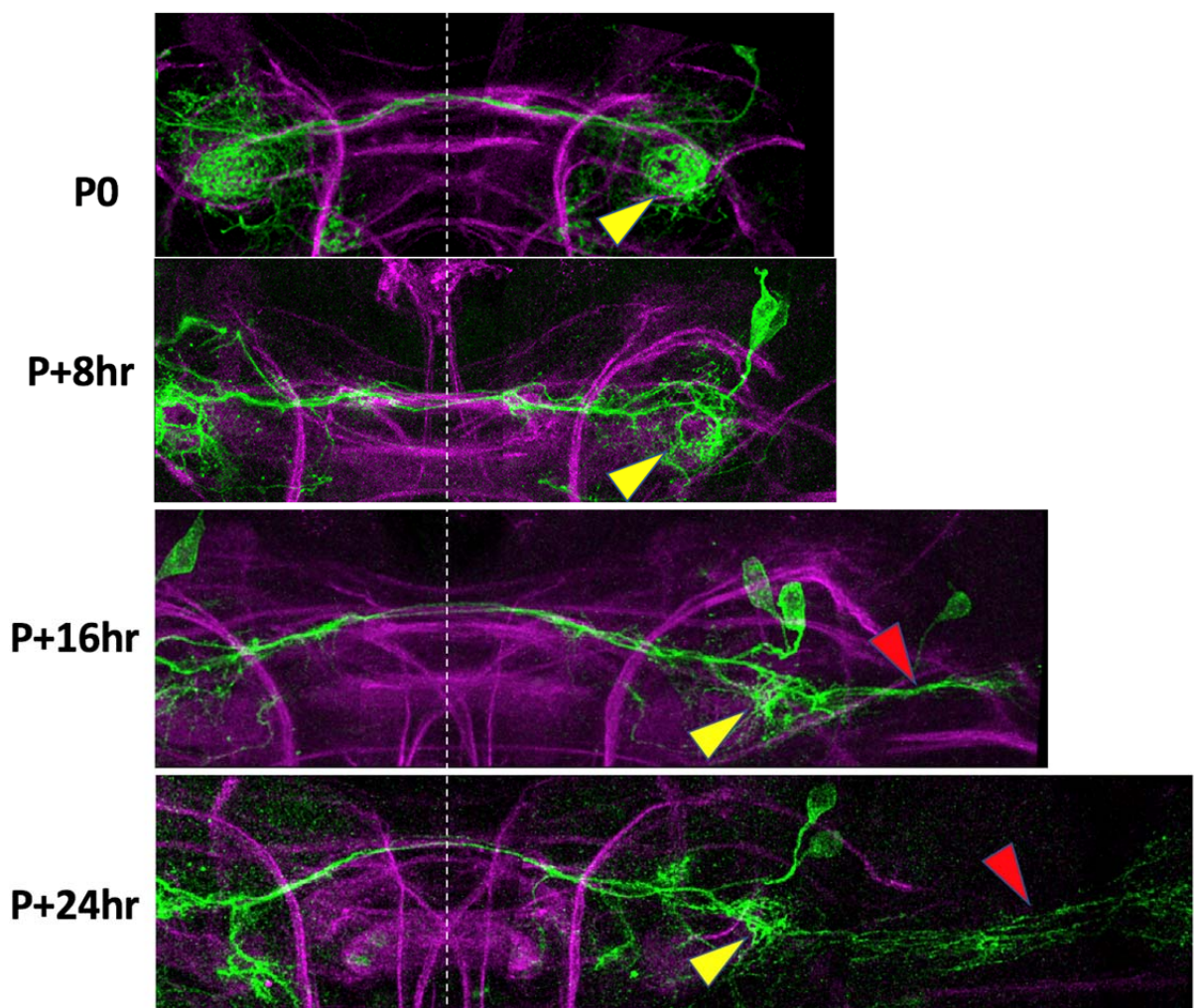


1285  
1286

1287 **Figure 2---figure supplement 2.** Confocal projections showing the terminal, adult identity of  
1288 larval MBINs that undergo trans-differentiation at metamorphosis. **(A,B)** female and male  
1289 versions of larval MBIN-b1 &-b2. Images to the right are a horizontal section at the level of the  
1290 tick marks showing that in males the cell innervates the medulla (med) but in the female the  
1291 medulla projection is reduced but it has extensive branching in the lobula (lob). Ot: optic  
1292 tubercle. **(C)** Frontal projection showing the terminal adult morphology of larval cell OAN-e1.  
1293 Image to right is a lateral section at level of the tick marks showing that the arbor is outside of  
1294 the bundles of Kenyon cell axons. C' and C'' are frontal slices at levels to relationship of arbor to  
1295 the  $\gamma$ ,  $\beta$ ' and  $\beta$  lobes of the medial lobes (C') and the  $\alpha$  and  $\alpha'$  lobes of the vertical lobes (C'').  
1296 **(D)** terminal adult anatomy of larval DAN-f1. **(E)** Terminal adult identity of larval MBIN-11.  
1297 Green: pseudo color representation of RFP; Magenta: nc82.  
1298  
1299



1300  
1301 **Figure 3---figure supplement 1.** Confocal projections showing the terminal, adult identity of  
1302 larval MBONs that undergo trans-differentiation at metamorphosis. Frontal views of the adult  
1303 brain showing the terminal identity of (A) MBON-d2, (B) MBON-b1 and -b2, (C) MBON-g1  
1304 and g2. (C') a magnified image of the boxed region of "C" showing the terminals of the neuron  
1305 in the intermediate section of the nodulus. Green: pseudo color representation of RFP; Magenta:  
1306 nc82.  
1307  
1308



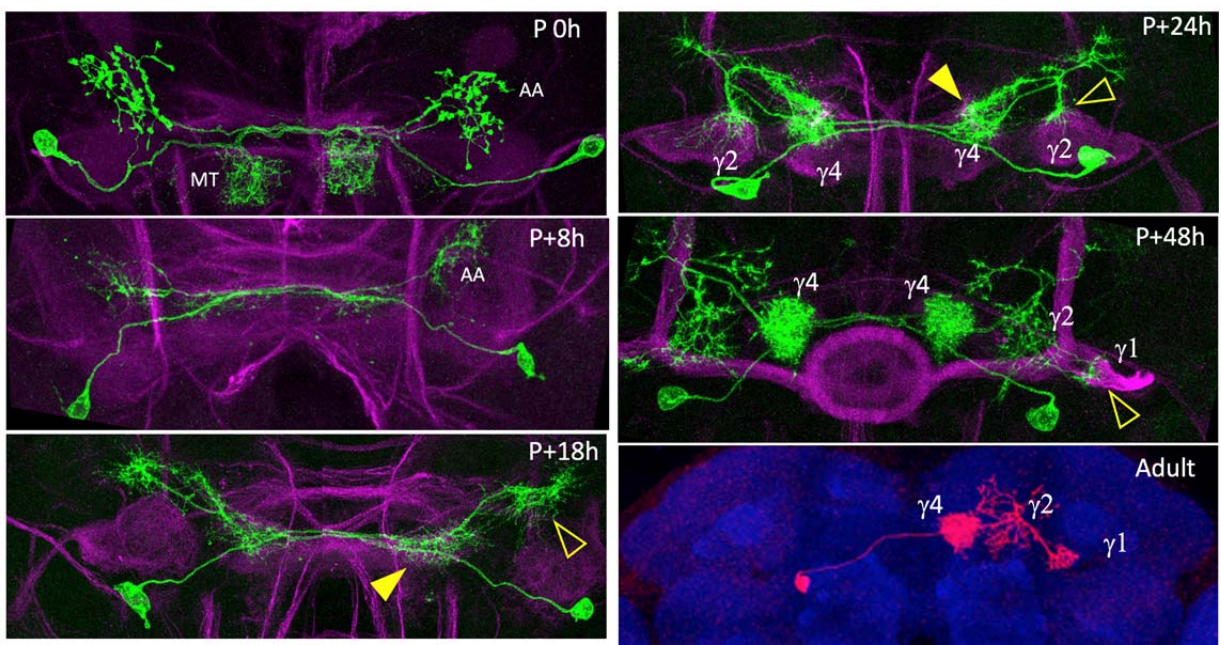
1309

1310

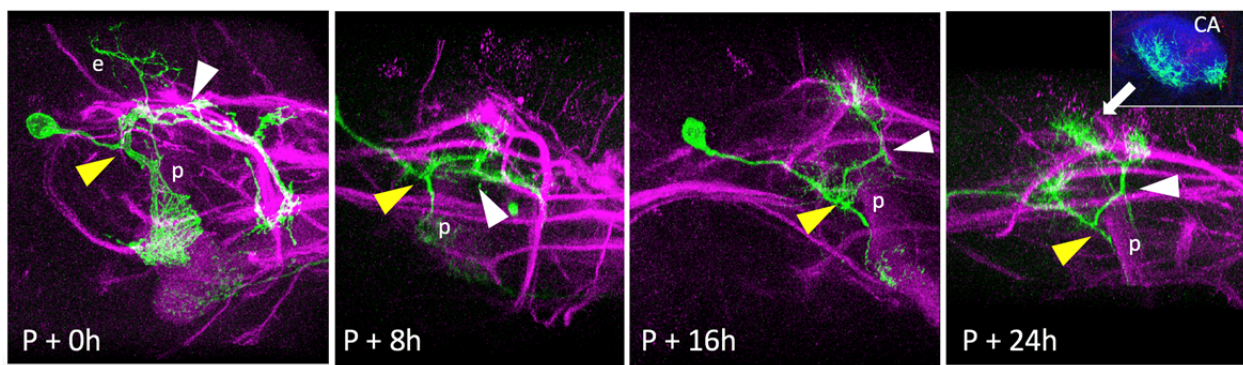
1311 **Figure 4---figure supplement 1.** The early metamorphic development of MBIN-b1 & -b2 in  
1312 hours after pupariation (P0). The yellow arrowhead marks the site where the larval cells invade  
1313 the intermediate peduncle. The red arrowhead marks the outgrowth into the optic lobe. Green:  
1314 Green Fluorescent Protein; magenta: fasciclin II.

1315

1316



1317  
1318 **Figure 5---figure supplement 1.** Pruning and outgrowth of MBON-j2 as it transforms into its  
1319 adult form named MBON 05. At pupariation (P 0h), MBON-j2 has a dendritic arbor in the  
1320 ipsilateral medial toe (MT) compartment and a contralateral axon arbor (AA). By P+8 hours, the  
1321 dendritic arbor is gone and the axonal arbor has severely reduced. At P+18 hours the cell has  
1322 formed contralateral outgrowth areas for new dendritic (filled arrowhead) and axonal arbors  
1323 (open arrowhead). P+24 h: dendritic growth invades the  $\gamma 4$  compartment (filled arrowhead)  
1324 while the axonal region splits into multiple growth cones, one of which invades the  $\gamma 2$   
1325 compartment (open arrowhead); By P + 48hr, a dendritic tuft fills the  $\gamma 4$  compartment and axonal  
1326 arbor is in  $\gamma 2$ , but the cell shows the delayed invasion of  $\gamma 1$ . Adult version of the cell is an Red  
1327 Fluorescent Protein version obtained by flip-switch treatment of MBON-j2 in the larva. Blue:  
1328 nc82; Green: Green Fluorescent Protein; magenta: fasciclin II.  
1329



1330  
1331

1332 **Figure 5---figure supplement 2.** Early stages in the metamorphosis of MBON-c1. This  
1333 example of MBON-c1 has an atypical ectopic branch (e) that leads to the larval calyx. Most  
1334 larval cells lack this branch. Subsequent images show the progression of arbor loss and  
1335 outgrowth through the 24 hours after pupariation. The yellow and white triangles show  
1336 comparable junctions in the cell through time. The inset at P+24 hr is a sub-stack projection  
1337 through the calyx (CA) neuropil showing growth cones invading this neuropil. p: peduncle;  
1338 green, Green Fluorescent Protein; magenta: fasciculin II; blue: N-cadherin.  
1339  
1340  
1341  
1342  
1343  
1344  
1345

1346 **Titles and Legends for Source Data Images.**  
1347  
1348 **Figure 2 – source data 1.** Examples of the adult anatomies of larval neurons MBIN-b1 and -b2 obtained  
1349 by flip-switch mediated immortalization of expression of line SS21716 late in larval life.  
1350  
1351 **Figure 2 – source data 2.** Examples of the adult anatomies of larval neurons DAN-c1 and DAN-d1  
1352 obtained by flip-switch mediated immortalization of expression of lines MB586B and MB328B,  
1353 respectively, late in larval life.  
1354  
1355 **Figure 2 – source data 3.** Examples of the adult anatomy of larval neuron OAN-e1 obtained by flip-  
1356 switch mediated immortalization of expression of lines SS21716 and SS01958 late in larval life.  
1357  
1358 **Figure 2 – source data 4.** Examples of the adult anatomies of larval neurons MBIN-l1 and DAN-f1  
1359 obtained by flip-switch mediated immortalization of expression of stable spilt lines late in larval life. The  
1360 anatomy of the adult form of MBIN-l1 was revealed using lines SS04484 and SS01624; that of DAN-f1  
1361 using lines MB065B and MB145B.  
1362  
1363 **Figure 2 – source data 5.** Examples of the adult anatomies of larval neurons DAN-g1 and OAN-g1  
1364 obtained by flip-switch mediated immortalization of expression of stable spilt lines late in larval life. The  
1365 anatomy of the adult form of DAN-g1 was revealed using lines SS017164 and SS01755; that of OAN-g1  
1366 using lines SS20844 and SS4268.  
1367  
1368 **Figure 2 – source data 6.** Table showing the success rate for maintaining expression of the various  
1369 larval neurons through metamorphosis.  
1370  
1371 **Figure 3 – source data 1.** Examples of the adult anatomy of larval neuron MBON-a1 obtained by flip-  
1372 switch mediated immortalization of expression of lines SS01417 and SS00867 late in larval life. The first  
1373 line also revealed an occasional adult form of MBON-a2  
1374  
1375 **Figure 3 – source data 2.** Examples of the adult anatomies of larval neurons MBON-a2 and MBON-b1,-  
1376 b2 obtained by flip-switch mediated immortalization of expression of stable spilt lines late in larval life.  
1377 The anatomy of the adult form of MBON-a2 was revealed using lines SS00872 and SS02006; that of  
1378 MBON-b1,-b2 using lines SS01708 and SS01959  
1379  
1380 **Figure 3 – source data 3.** Examples of the adult anatomies of larval neurons MBON-d1, MBON-e2 and  
1381 MBON-f2 obtained by flip-switch mediated immortalization of expression of stable spilt lines late in  
1382 larval life. The anatomy of the adult form of the three neurons was revealed using lines SS01705,  
1383 SS04172, and SS04328, respectively.  
1384  
1385 **Figure 3 – source data 4.** Examples of the adult anatomies of larval neurons MBON-g1 and -g2 obtained  
1386 by flip-switch mediated immortalization of expression of lines SS02130 and SS02121 late in larval life.  
1387  
1388 **Figure 3 – source data 5.** Examples of the adult anatomies of larval neurons MBON-h1 and -h2 obtained  
1389 by flip-switch mediated immortalization of expression of line SS01725 late in larval life.  
1390  
1391 **Figure 3 – source data 6.** Examples of the adult anatomies of larval neurons MBON-j1 and MBON-j2  
1392 obtained by flip-switch mediated immortalization of expression of lines SS01973 and SS00860 late in  
1393 larval life.  
1394  
1395 **Figure 3 – source data 7.** Examples of the adult anatomies of larval neurons MBON-i1 and MBON-k1  
1396 obtained by flip-switch mediated immortalization of expression of lines SS01962 and SS04236 late in  
1397 larval life.

1398 **Figure 4 - source data 1.** Examples of the adult anatomies of larval neuron APL obtained by flip-switch  
1399 mediated immortalization of expression of line SS01671 late in larval life.

1400

1401

1402

1403

1404

1405